UNIVERSITY OF OKLAHOMA

GRADUATE COLLEGE

BIOMOLECULAR PRESERVATION IN DENTAL CALCULUS FROM THE TEOTIHUACAN RITUAL LANDSCAPE

A THESIS

SUBMITTED TO THE GRADUATE FACULTY

in partial fulfillment of the requirements for the

Degree of

MASTER OF ARTS

By

STERLING LEE WRIGHT

Norman, Oklahoma

2019

BIOMOLECULAR PRESERVATION IN DENTAL CALCULUS FROM THE TEOTIHUACAN RITUAL LANDSCAPE

A THESIS APPROVED FOR THE DEPARTMENT OF ANTHROPOLOGY

BY

Dr. Courtney Hofman, Chair

Dr. Krithivasan Sankaranarayanan

Dr. Matthew Pailes

Acknowledgements

I am grateful for the support from my committee members throughout this project. I thank Dr. Matthew Pailes for his guidance about archaeology in the Americas. I thank Dr. Krithivasan "Krithi" Sankaranyayanan for his instruction and affirmation that I understand the bioinformatic analyses applied within this project. Above all, I am most grateful to be under the tutelage of Dr. Courtney Hofman who provided me an opportunity when no one else did. Her guidance and mentorship significantly integral to my development as a scholar. In addition, I thank the faculty and staff of the Department of Anthropology for making me a better graduate student. I also thank Dr. Tanvi Honap for her bioinformatic pipelines that truly helped me during this project. I am also grateful for John Boyd and Elizabeth Young for their efforts in making LMAMR one of the best laboratories in the world. I am especially thankful for Nihan Dagtas and Karissa Hughes who were instrumental for the lab work for this project. Finally, I was truly blessed to have such wonderful lab mates who were monumental in the completion of this project. Justin Lund, Rita Austin, Jacob Hafner, Abigail Gamble, Kristen Rayfield, Robin Singleton, Nisha Patel, Christine Woelfel-Monsivais, and especially David "Dave" Jacobson. It cannot be understated how grateful I am for Dave's patience and knowledge about the microbiome field enhanced the quality of this project. I am also compelled to thank Cellar Darling, Avenged Sevenfold, Kate Voegele, and all the other artists on my iPod. Let this thesis be a testament to art being an impetus for science. For this reason, this project would not have been possible without the efforts of so many people.

Table of Contents

List of Tables

List of Figures

Abstract

The advent of high-throughput sequencing techniques has yielded a wealth of genomic information about the human oral microbiome. This research has expanded with the direct sequencing of DNA from dental calculus (calcified dental plaque) from archaeological material. Archaeological dental calculus is a biomineral that contains remnants of the oral (subgingival) microbiome. While preserved DNA in dental calculus has been characterized from a number of archaeological contexts, similar research in Mesoamerica is needed. This study aims to provide empirical data about biomolecular preservation in Mesoamerican dental calculus by performing DNA sequencing on dental calculus recovered from the Plaza of the Columns Complex and the Moon Pyramid, two archaeological contexts at Teotihuacan. DNA was extracted using a modified Dabney et al. (2013) protocol. The extracts were built into high-throughput (Illumina) shotgun sequencing libraries. Quality filtered sequences were analyzed to evaluate overall DNA preservation (microbial and host), and characterize microbial community profiles. While the samples selected from the Moon Pyramid (n=3) showed strong evidence of post-depositional environmental contamination, a well-preserved microbial community was identified from the Plaza of the Columns sample (n=1). Therefore, this thesis suggests the recovery of biomolecules from a Mesoamerican context varies within a site and that dental calculus is susceptible to taphonomic processes.

Introduction

Project Summary:

- To assess the biomolecular preservation of dental calculus from two archaeological contexts at Teotihuacan, we conducted a high-throughput sequencing study on four dental calculus samples.
- To assess the microbial community diversity, we applied two commonly-used microbiome analysis pipelines targeting distinct taxonomic markers: QIIME and MetaPhlAn.
- To assess ancient DNA (aDNA) preservation, we applied three different authentication criteria: SourceTracker (microbial community profile), fragment length distribution and MapDamage (microbial and host DNA preservation).

In 2007, the National Institute of Health established the Human Microbiome Project (HMP) to identify and characterize the human microbiome—the aggregate DNA content of microbes coexisting within the human body (Turnbaugh et al., 2007). Since the inception of HMP, the study of the microbiome in conjunction with advances in sequencing technology have reshaped our understanding how microbes impact human health and disease (Benn et al., 2018; Giongo et al., 2011; Gomez-Arango et al., 2016; Ojeda-Garcés et al., 2013). For instance, high-throughput sequencing (HTS) technologies and bioinformatic methods have shown us how the composition and functional capacity of microbial communities in the gut can influence several diseases (Dave et al., 2012). Similar research on the microbial communities within the mouth has lagged behind (Zaura et al., 2014).

The oral microbiome

The human oral cavity encompasses a dynamic and diverse microbial community (Marsh et al., 2009). The HMP found that 185-355 genera, belonging to 13-19 bacterial phyla, dominate the oral microbiome (Zhou et al., 2013). Of these phyla, approximately 700 oral bacterial species dominate the oral microbiome (Benn et al., 2018; Wade, 2013). Some of these species play a role

in the development of periodontal, respiratory, neurological, cardiovascular and systemic diseases (Dewhirst et al. 2010; Huttenhower et al. 2012; Hujoel 2009; Leishman, Lien Do, and Ford 2010; Paranjapye and Daggett 2018). In addition to a wide-array of taxa, the oral cavity is also comprised of several ecological niches—teeth, the gingival sulcus, the attached gingiva, the tongue, the cheek, the lip, and the hard and soft palate, and saliva—and each promotes the development of different microbial communities.

Dental plaque, an oral biofilm, is the accumulation of microbes on the tooth surface near the gingival margin and in the gingival sulcus (Struzycka, 2014). A number of species within this biofilm play an active role in the development and pathogenesis of oral diseases, including caries, gingivitis, and periodontitis (Mancl et al., 2013). For instance, *Streptococcus mutans*, a species that is commonly found in dental plaque, manufactures lactic acid which degrades enamel (Gao et al., 2016; Ojeda-Garcés et al., 2013; Okada et al., 2003; Simón-Soro and Mira, 2015).

Another example of a dental biofilm is dental calculus. Even though the exact mechanisms for dental calculus formation is unknown, dental calculus is formed when dental plaque, saliva, gingival crevicular fluid, and calcium phosphate minerals are present (Warinner et al., 2014). Dental calculus formation may also incorporate other particles, such as airborne and waterborne pollutants, plant and animal fibers, dietary microfossils, and the DNA from hosts and microbes (Warinner et al., 2015). HTS of archaeological dental calculus provides a critical source of information about the oral microbiome of past populations. This application in turn has enabled the study of variation and evolution of the oral microbiome.

Dental calculus and ancient oral microbiomes

Dental calculus is a source of oral health and subsistence strategies from past populations (Warinner et al., 2015). The earliest studies on archaeological dental calculus focused on faunal diet reconstruction (Armitage, 1975; Brothwell, 1981; Rowles, 1961). Well-preserved organic materials, such as pollen grains, animal hair, and a variety of unidentifiable animal and plant tissues have also been recovered from faunal dental calculus (Dobney and Brothwell, 1988, 1986). The same techniques have been applied to human dental calculus and as a result enabled the study of archaeological dental calculus to also focus on human diet reconstruction (Hansen and Medlgaard, 1991; Lilley, 1994). While Dobney and Brothwell (1988) observed and described calcified oral microbes by using a scanning electron microscope, they were unable to identify a specific oral species.

In 1996, Linossier's et al.'s (1996) immunohistochemical analysis of dental calculus marked the first biomolecular investigation of archaeological dental calculus and was able to identify *S. mutans* (Linossier et al., 1996). In 2011, transmission electron microscopy confirmed the preservation of bacterial DNA within archaeological dental calculus (Preus et al., 2011). This finding was supported when PCR-based genetic approaches recovered DNA of *S. mutans* and other oral taxa from archaeological dental calculus (De La Fuente et al., 2013). However, there are several limitations to PCR-based approaches. One limitation of PCR is that it generally requires DNA templates that are longer than 100 base pairs (bp) which is often not the case for most authentic ancient DNA (aDNA) sequences (Pääbo et al., 2004; Sawyer et al., 2012). Second, aDNA can require more than 35 PCR cycles for successful target amplification which also increases the risk of amplifying background and environmental contamination (Wintzingerode et al., 1997). Third, the nature of cloning and Sanger sequencing limit the investigation of template damage patterns (Hofreiter et al., 2015). Fourth, targeted PCR is

susceptible to amplification biases, including both off-target and skewed PCR amplification (Suzuki and Giovannoni, 1996). Fifth, aDNA scholars have been unable, at times, to replicate their findings using PCR (Pääbo et al., 2004; Poinar and Cooper, 2000; Stoneking, 1995). Thus, while this early PCR-based study on dental calculus paved the way for ancient oral microbiome research, it only provided a low-resolution survey of the microbial community present.

The advent of HTS technologies revolutionized the study of DNA within dental calculus by providing high-resolution taxonomic profiles of microbial communities. In 2013, 16S rRNA amplicon sequencing of 34 dental calculus samples spanning from the Mesolithic to the present generated the first ancient oral microbiome HTS profiles (Adler et al., 2013). At the time, a finding in this study proposed that changes in the microbial diversity of dental calculus reflected the development of subsistence strategies, namely agriculture and industrialization. However, these inferences have been questioned due to amplification biases in 16S rRNA amplicon sequencing and due to preservation bias in dental calculus (Ziesemer et al., 2015).

Following Adler et al., Warinner et al. (2014) employed an even higher resolution microbial community survey by using shotgun metagenomics, another HTS application, and metaproteomics on four Medieval dental calculus samples from Germany. They demonstrated that applying a shotgun-based approach allowed characterization of an ancient oral microbiome in a diseased state, recovered opportunistic pathogens as well as human-associated putative antibiotic resistance genes, and facilitated reconstruction of a pathogen genome associated with periodontal disease. Moreover, they demonstrated that dental calculus may retain up to a thousandfold more DNA than bone with most of it being microbial. Since then, several other dental calculus studies have been published using HTS technology and have been verified with

several authentication methods (Mann et al., 2018; Moorhouse et al., 2015; Ozga et al., 2016; Sawafuji et al., 2018; Weyrich et al., 2017).

History of authenticating ancient DNA

Authenticating aDNA has remained a persistent challenge in the field since its inception in the 1980s (Pääbo, 1985; Pääbo et al., 2004). For example, Austin et al. (1997) reported how aDNA scholars studying dinosaur remains were unable to replicate results (Golenberg et al., 1990; Soltis et al., 1992; Woodward et al., 1994). A similar issue would arise as scholars began to analyze human aDNA because it was difficult to differentiate endogenous and exogenous content (Stoneking, 1995). The reoccurrence of this issue in the 1990s led Poinar and Cooper (2000) to publish an outline of nine key standards that minimized contamination. Despite their efforts, few studies applied all nine standards (Gilbert et al., 2005). However, technological advancements in HTS sequencing, (Schuster, 2007), contamination control (Champlot et al., 2010), laboratory setup (Gilbert et al., 2005; Knapp et al., 2012), and the furtherance of bioinformatic applications tailored for aDNA research have enabled researchers to empirically test DNA preservation and levels of contamination of ancient samples, including archaeological dental calculus. For instance, HTS (untargeted) approaches have enabled the recovery of short DNA fragments (<100 bps) within a sample. Novel strategies to recover endogenous content have also increased the chances of success (Dabney et al., 2013). Bioinformatic tools, such as MapDamage and SourceTracker, have also provided additional strategies to authenticate aDNA (Ginolhac et al., 2011; Jónsson et al., 2013; Knights et al., 2011).

Many aDNA studies employ MapDamage as a tool to quantify DNA preservation in their samples (Allentoft et al., 2015; Hofreiter et al., 2015; Rasmussen et al., 2015; Seguin-Orlando et al., 2014). MapDamage utilizes a Bayesian framework that models *postmortem* damage in DNA

molecules. In theory, DNA strands accumulate breaks because the enzymes involved in DNA repair *in vivo* no longer function once an organism dies (Briggs et al., 2007; Dabney et al., 2013b; Green et al., 2009). The degree of damage is also impacted by environmental factors. Research has shown that the thermal age, the pH level and temperature of the soil, sample excavation and storage practices, and species and tissue types can also potentially the impact the fragmentation and decay rates of DNA (Kistler et al., 2017; Mitchell et al., 2005). However, the fragmentation of DNA is not stochastic. Empirical research shows that aDNA has increased cytosine deamination rates at 5'—overhangs, resulting in an increase in C→T substitution rates toward the 5' end of the molecule and consequently have an increased rate of G→A substitutions toward the 3' end of the molecule (Briggs et al., 2007). This model is applied in MapDamage and has enabled the comparison of DNA damage patterns of ancient datasets derived from various temporal and spatial contexts.

Another authentication method is SourceTracker, which also applies Bayesian-based statistics (Knights et al., 2011; Tito et al., 2012). The tool utilizes taxonomic inventories generated from HTS data, and models the proportion of well-characterized environments or "source communities" (e.g. skin, gut, oral, laboratory, and soil) in an ancient substrate or "sink" such as a dental calculus sample. In addition to known sources, sinks can also have high "unknown" proportions, which is common since many of the microbes within an ancient sample may be uncharacterized or may occur in more than one environment (Tito et al., 2012). The efficacy of this bioinformatic tool to predict contamination has been well-demonstrated within ancient microbiome samples (Mann et al., 2018; Warinner et al., 2014).

These technological developments as well as the increased number of aDNA studies have led some scholars to agree that the field has entered into its "golden age" (Poinar in Culotta

2015). However, the lack of protocol standardization within the study of dental calculus and coprolites has some scholars uncertain about which ones are the most robust as well as the authenticity of the studies (Warinner et al., 2017). For instance, Santiago-Rodriguez et al. (2016) characterized the gut microbiome of Andean mummies dating to the 10^{th}-15^{th} centuries using 16S rRNA gene sequencing strategies. A reply to the editor noted that Santiago-Rodriguez and colleagues neglected to properly authenticate their ancient bacterial DNA (Eisenhofer et al., 2017). Eisenhofer et al. questioned the use of agarose gels and the lack of including sequence data from extraction blank controls during the library amplification process. They state that agarose gels lack the sensitivity to detect bacterial contaminants present in extraction controls and the samples. Furthermore, they explain that Santiago-Rodriguez et al. did not report the reference sequence used for their MapDamage results. In theory, since the samples utilized in the study were coprolites, Santiago-Rodriguez et al. should have used a well-characterized gut microbe to authenticate their DNA. If they were to use a skin or oral microbe, the deamination rates would likely be different.

Toranzos, a co-author in the original study, and colleagues (2017) responded to Eisenhofer et al. by contending that there was no possibility of their reagents having contamination because they were kept in sterile environments. They also justified their use of agarose gels as a method for detecting contamination. Toranzos et al. also note that their genomes may "remain undegraded over millennia, if these ancient microorganisms were rapidly dehydrated, as is the case of the process of natural mummification." However, the authors fail to cite any sources to support these arguments. Previous research would strongly suggest that reagent and laboratory contamination is always a risk and that the degradation of DNA occurs

regardless of environment, thermal age and geographic origin (Hofreiter et al., 2015; Salter et al., 2014).

In order to resolve the lack of standardization in the study of ancient microbiomes, Warinner et al. (2017) provided a framework for ancient microbial research. This framework provided specific standards and guidelines that ranged from the equipment necessary to minimize contamination to the bioinformatic applications for assessing contamination and preservation. While these guidelines are informative and provide a roadmap for research on ancient substrates, there still needs empirical work to identify baseline patterns for dental calculus. Some of this effort has already started—Mann et al. (2018) employed HTS to paired dental calculus and dentin samples from 48 individuals spanning a number of regions and time periods across Europe, North America, and Asia. Their results suggested that the DNA in dental calculus is more abundant and less prone to contamination than the DNA in dentin. This global dataset along with ones from previous studies show that human-associated oral taxa dominate the microbial communities of dental calculus, whereas environmental sources dominate dentin (Warinner et al., 2014; Weyrich et al., 2017). In addition, Mann et al. (2018) found that the human DNA fragments obtained from dental calculus are on average shorter than the microbial DNA fragments in a paired dentin sample. Thus, Mann et al. found broadly consistent patterns across multiple archaeological contexts. However, their findings may not be found in other contexts where there is a history of taphonomic and post-depositional processes inhibiting aDNA research.

Ancient DNA research in Mesoamerica

Mesoamerica refers to a group of cultures that shared a suite of characteristics, including intensive agriculture, stone pyramids, ball courts, hieroglyphic writing, a calendrical system, and

the practice of human sacrifice (Kirchhoff, 1952). Genetics research on Mesoamerican cultures have been stymied due to the unfavorable environmental conditions for DNA preservation (Chatters et al., 2014; Mendisco et al., 2015; Schroeder et al., 2015). Nevertheless, successful aDNA studies have provided a glimpse of the population history of Mesoamerica prior to European contact. For instance, aDNA studies support that Mesoamerican populations had high frequencies of haplogroup A and moderate to low frequencies of haplogroup B (Álvarez-Sandoval et al., 2015; González-Oliver et al., 2001; Kemp et al., 2010; Merriwether et al., 1997). However, most studies have only been able to partially reconstruct mitochondrial genomes (mitogenomes) in Mesoamerica (Raff et al., 2011). HTS strategies have changed this narrative by reconstructing mitogenomes and whole genomes of Mesoamerican individuals (Álvarez-Sandoval et al., 2015; Morales-Arce et al., 2019; Morales-Arce et al., 2017). However, several Mesoamerican populations still remain unstudied.

Situated in the Central Mexican highlands (Figure 1), the Teotihuacano culture had considerable influence throughout Mesoamerica during the Classic period (150-650 CE) (Robb, 2017). In this period, the population of Teotihuacan supported more than 100,000 inhabitants who lived in different social and spatial units (Manzanilla, 2015). Current genetic evidence supports the notion that Teotihuacan was a multiethnic center (Álvarez-Sandoval et al., 2015). One such extra-local group are inferred to be Maya from lowland Mesoamerica to the south of Teotihuacan. Even though these two cultures dominated the Mesoamerican landscape during the Classic period, the socio-political relationships between them remain in question (Robb, 2017). For instance, scholars are still not certain about the relationships between Maya elites and Teotihuacanos (Carballo et al., 2018; Robb, 2017; Sugiyama et al., 2016). Genetic studies could potentially elucidate these relationships but destructive analyses of skeletal remains are not

always a viable option for aDNA research. Dental calculus from Mesoamerican contexts may serve as an alternative source for host DNA. Recent studies have shown that it is possible to obtain genomic-scale information from host DNA within dental calculus despite low abundance (Ozga et al., 2016; Ziesemer et al., 2019).

Research Objectives

In the present study, shotgun metagenome sequencing is utilized to characterize host and microbial DNA preserved in dental calculus from Teotihuacan. The host DNA was of special interest due to the unique burial context for each Teotihuacan sample. Preservation of host and microbial DNA in these samples is compared to patterns reported from previously published studies of dental calculus obtained from other spatial and temporal contexts (Mann et al., 2018; Weyrich et al., 2017). In addition, this study aimed to see whether there were sufficient host DNA within the four dental calculus samples to determine ancestry. The four individuals within this current study represent two Classic period sites—three individuals from burial 5 of the Moon Pyramid (PPL) and one individual from Front A of the Project Plaza of the Columns Complex (PPCC). The contexts of these four samples suggest connections with Maya populations. This led the archaeologists at the site to become interested in evaluating the possibility of reconstructing their ancestry. However, first the DNA preservation was evaluated to assess the viability of further work. The DNA preservation of the Teotihuacan samples was determined using four main measures: (1) microbial composition and abundance, (2) microbial DNA damage and fragmentation patterns, (3) human DNA content, and (4) human DNA damage and fragmentation patterns. The results indicate that the microbial profiles of the PPCC sample retained a robust signal of the human oral microbiome, whereas the PPL samples yielded soil and skin signatures. Although a considerable amount of human DNA was found in the PPL samples,

findings from MapDamage and fragmentation analyses indicate that they are modern contaminants. Thus, the results of this study strongly indicate that the microbial and human DNA in the PPCC sample preserved better than the PPL samples.

Figure 1. Satellite image of Central America. Site locations discussed in the text. The figure was generated with ArcGIS 10.4 software (http://www.esri.com/software/arcgis). Service layer credits Imagery. I acknowledge the use of satellite and aerial imagery from the USGS.

Materials and Methods

Archaeological site and samples

Between 1 CE and 650 CE the people of Teotihuacan built ceremonial precincts, monumental pyramids, ornate temples, communal areas, exchange sectors, and residential compounds (Price et al. 2000). Among these structures were the Moon Pyramid and the Plaza of the Columns Complex, both of which date to the Classic period (Figure 2). Dental calculus from several individuals in these two contexts were subsampled in July 2017 by Dr. Courtney Hofman. The Moon Pyramid samples (n=3) were excavated during the 1998-2004 field seasons (Sugiyama and Castro, 2007) while the Plaza of the Columns sample (n=1) was excavated during the 2017 season (Carballo et al., 2018). Both structures served as ceremonial precincts—the Moon Pyramid was a venue for religious events while the Plaza of the Columns was an administrative structure (Carballo et al., 2018; Sugiyama and Castro, 2007).

Three of the four dental calculus samples in this study came from burial 5 of the Moon Pyramid. Archaeologists at the Moon Pyramid unearthed a series of earlier versions of the structure, as well as burials in the form of ritual offerings (Sugiyama and Luján, 2007). Sugiyama and Luján report six distinct burials, each associated with a different construction phase. The archaeological contexts suggest the skeletons in burials 1-4 and 6 were interred as sacrifices, burial 5 remains ambiguous. They report that burial 5 appeared undisturbed from later alteration or looting likely due to thick fill. Burial 5 includes three complete human skeletons (PPL 5A, PPL 5B, and PPL 5C) along with pumas, rattlesnakes, an eagle, and a variety of offerings (Sugiyama and Luján, 2007).

Each human remain was seated facing west and in the lotus position, with their hands together in front and resting above their feet (Pereira et al., 2003). According to Sugiyama and Luján (2007), the individuals were willingly bound and buried since there were no signs of

struggle. An analysis of the sacra and ossa coxae of PPL 5A, PPL 5B, PPL 5C indicate that the individuals were male between the ages of 50-70, 40-50, and 40-45 years old (Spence and Pereira, 2007). In addition, almost identical emerald green jade pectoral chest ornaments adorned PPL 5A and _5B, who were seated juxtaposed near the west wall. From the Early and into the Late Classic, only the upper elite of the Maya society had access to these style of glyphs (Hammond et al., 1977; Taube, 2005). Since the anatomical positions and grave goods of the individuals in burial 5 are not observed in other Teotihuacan burial contexts, these individuals likely had special status (e.g. rulers, ambassadors, warriors, or merchants) who either had close connections with Maya dynasties or were members of the Maya elite (Pereira et al., 2004).

One dental calculus sample came from non-burial fill within Front A of the Plaza of the Columns Complex (PPCC). The PPCC represents a civic-administrative structure and includes the largest three-temple complexes with the fourth highest pyramid, a main plaza (11,408 m^2), and occupational layers that may date to the earliest urban foundations at Teotihuacan (Sugiyama et al., 2016). The PPCC is divided into five fronts (A, B, C, D, E, and F) with Front A, where the PPCC sample was excavated, comprising the southern sector. Ongoing excavations at PPCC have also unearthed sculptural motifs in the Maya style illustrating the strong relationships between Teotihuacan and Maya city-states.

DNA Extraction

Four dental calculus samples were collected at Teotihuacan in summer of 2017. These samples were processed in a dedicated ancient DNA laboratory at the Laboratories of Molecular Anthropology and Microbiome Research (LMAMR) in Norman, Oklahoma, USA. Appropriate non-template controls were included during the extraction and shotgun library build process. DNA extraction was performed following a modified Dabney et al. 2013 protocol. In brief, ~3.6-

10.1 mg of calculus was gently rotated in 1 ml of 0.5 M EDTA for 15 minutes to remove surface contamination. Following pulverization, the samples were demineralized in a solution of 0.5M EDTA at room temperature overnight and 100 µl 20 mg/ml Proteinase K (Qiagen) was added the next day. Samples were incubated at room temperature for 4 days—until complete digestion. DNA was isolated using a column-based purification method eluted in 60 µl of EB buffer (Qiagen) and quantified using a Qubit 3.0 fluorometer.

Illumina library preparation and sequencing

Approximately 86.8 ng of DNA from the PPCC sample and an unknown quantity of DNA from PPL samples (<.01 ng) were used for shotgun Illumina library construction following Carøe et al. 2018 (with minor modifications). End repair was performed using 16 µl reactions—consisting of T4 DNA ligase reaction buffer, dNTPs, T4 PNK, and T4 DNA polymerase—with 14 µl of DNA extract and was incubated for 30 min at 20° C and 30 min at 65° C. Following end-repair, Illumina adapters were ligated in 20 µl reactions with 1 µl of BEDC3 adapter mix (28.14 µM). Reactions were incubated for 30 min at 20° C and for 10 min at 65° C followed by 20 min at 80° C. For adapter fill-in, Isothermal amplification buffer, dNTPs, water, and Bst 2.0 Warmstart Polymerase were incubated for 20 min at 65° C and for 20 min at 80° C in a final volume of 30 µl (Carøe et al., 2018). The reactions were purified using modified Speedbeads (Rohland and Reich, 2012). A quantitative PCR (qPCR, Lightcycler 480 Roche) was performed on each sample to evaluate the amount of DNA present in each library. Libraries were amplified in triplicate 25 µl PCR reactions using 4 µl template, 12.5 µl of a 2x KAPA HiFi HotStart Ready master mix, 6 µl H20, 1.5 µl DMSO, 1 µl BSA (2.5 mg/ml), and 0.75 µl each of barcoded forward and reverse indices (10 µM). Thermocycler conditions were 5 min at 95° C followed by a 12-25 cycles of 20 seconds at 98° C, 15 seconds at 60° C, and 30 seconds at 72° C, followed by

a final elongation step for 1 minute at 72° C. Pooled triplicate amplified libraries were then purified using Speedbeads and eluted in 30 µl EB. The libraries were quantified using quantitative PCR (qPCR, Lightcycler 480 Roche) and library size was estimated on a Fragment Analyzer. Libraries were pooled in equimolar ratios and a Pippin Prep was used to select DNA molecules between 150 to 500 bp. The pool was sequenced on an Illumina HiSeq 2500 using a paired-end, 2 x 150 bp, rapid-run chemistry at the Oklahoma Medical Research Foundation.

Shotgun data analysis and quality filtering

Low quality and adapter sequences were removed using AdapterRemoval (Schubert et al., 2016) with the following options: --trimns --trimqualities --minquality 20 --collapse --minlength 30. The resulting analysis-ready reads were used for downstream analyses.

Metataxonomic characterization

Analysis-ready reads from the 4 dental calculus samples were mapped to the Greengenes (v13.8) 16S rRNA gene database (DeSantis et al., 2006) using bowtie2 aligner (Langmead and Salzberg, 2012). SAMtools (v. 1.5) was then used to sort and de-duplicate the mapped reads. Reads that mapped to the greengenes database were assigned to operational taxonomic units (OTU) using QIIME (v. 1.9.1). Taxonomic binning was performed against the greengenes 16S rRNA gene database (version 13.8) preclustered at 97% sequence similarity with the pick_closed_reference_otus.py script and the following options: --max_accepts 500, max_rejects 500, --word_length 12, --stepwords 20, --enable_rev_strand_match True. The operational taxonomic unit (OUT) file was then rarefied to 1100 reads to explore metataxonomic diversity.

Additionally, Metataxonomic Phylogenetic Analysis (MetaPhlAn) (v. 2.7.7) was also used to estimate phylum, genus, and species abundance. Merged reads were taxonomically binned using the metaphlan2.py script. The script generated two files for each sample, one

containing reads that mapped to specific sequence markers and the other containing the relative abundances at each taxonomic level.

SourceTracker –a Bayesian approach to estimate endogenous and exogenous content

Potential source contribution to samples were calculated from rarefied genus-level bacterial and archaeal taxonomic frequency tables from QIIME using Sourcetracker version 0.9.8 (Knights et al., 2011). This analysis used comparative data from well-characterized source communities to predict source contributions to a given sample (Appendix Table A.1). Raw sequences were downloaded and processed in the same manner as the samples in the current study. These sources included ancient dental calculus (Mann et al., 2018; Weyrich et al., 2017), human gut (Gopalakrishnan et al., 2018; Rampelli et al., 2015), plaque (Lloyd-Price et al., 2017), saliva (Aleti et al., 2018; Lassalle et al., 2018), skin (Oh et al., 2016; Schmedes et al., 2016; Tirosh et al., 2018), and soil (DOE Joint Genome Institute, 2017; Lin et al., 2014). Additionally, ancient dental calculus samples—ElSidron1, ElSidron2, and OldSpy—were added as sources from Weyrich et al. (2017) and can be downloaded from https://www.oagr.org.au/.

Human DNA analysis

Analysis-ready reads were mapped to the hg 19 reference sequence (International Human Genome Sequencing Consortium, 2001). To determine mitochondrial haplotype, quality filtered reads were mapped to the human mitochondrial reference sequence (rCRS) (Anderson et al., 1981; Andrews et al., 1999). Categorization of mtDNA haplogroups was done using HaploGrep (http://haplogrep.uibk.ac.at/).

Ancient DNA authentication

Alignments resulting from mapping to the hg19, *Methanobrevibacter oralis*, *Streptococcus anginosus* and *Cutibacterium acnes* references were used to authenticate the recovery of ancient DNA molecules. *Methanobrevibacter oralis* was chosen as it exhibited high

relative abundance in the MetaPhlAn analysis and has also been well documented in dental calculus samples (Mann et al., 2018; Weyrich et al., 2017). *Streptococcus anginosus* was selected due to its presence in both the PPCC and PPL samples. *Cutibacterium acnes* was also chosen as it exhibited high relative abundance but also as a control since it is a well characterized skin bacterium (Chen et al., 2018; Oh et al., 2016). MapDamage 2.0 (Jónsson et al., 2013) was used to assess aDNA damage and fragmentation patterns. The relationships between DNA damage patterns, fragment length distributions, and other metadata were then visualized in R (version 3.5.2).

Figure 2. Aerial view of the Teotihuacan site. The Moon Pyramid is highlighted in blue and the area for the Plaza of the Columns is highlighted in purple. The Avenue of the Dead is demarcated with the bold white line and the Sun Pyramid is highlighted in yellow. Approximately 440 m separate the two areas. Both structures date to the Classic period (300-950 CE).

Results

Read Metadata

The mean number of reads generated for each sample, excluding negative controls, is 11,553,643 before quality filtering *(minimum=9,974,121, median=11,415,281.5, maximum=13,409,888)* (Table 1). The mean number of paired-end reads that successfully merged is 10,530,177 (*minimum=8,929,205, median=10,807,185, maximum=11,577,133*), which represents an average of 91.26% merged. The mean number of reads for the negative controls is 7,759,789.33 (*minimum=408,363, median=11,014,302, maximum=11,856,703*). The mean number of negative control paired-end reads that successfully merged is 7,094,963.33 (*minimum=12,007, median=11856703, maximum=11,856,703*). The library negative was omitted from downstream analysis due to less than 50 unique reads mapping to any reference.

Metataxonomic characterization

The microbial community for each sample and negative control was characterized with QIIME and MetaPhlAn. According to Huynh et al. (2016), there are 10 core phyla found in dental calculus: Bacteroidetes, Proteobacteria, Actinobacteria, Firmicutes, TM7, Synergistetes, Chloroflexi, Fusobacteria, Spirochetes, and Euryarchaeota. QIIME identified all ten of these phyla in the PPCC sample and at least 5 of the phyla in the PPL samples (Figure 3). The relative abundances for the top three most abundant in each sample are shown in Table 2. Several genus representatives that have been found in dental calculus include *Tannerella*, *Desulfobulbus*, *Actinomyces*, and *Streptococcus* and *Methanobrevibacter* (Dewhirst et al., 2010). QIIME OTU picking also showed that the PPCC sample had all of these genera. The PPL 5A was the only Moon Pyramid sample that had Streptococcus (Table 3). QIIME showed that the PPL samples had several genera mainly found in soil and skin microbiomes (e.g. *Acidobacteria* gen., *Solibacteraceae*, *Xanthomonadaceae* gen., and *Rhodospirillacea* gen.) (Chen et al., 2018; DOE

Joint Genome Institute, 2017; Oh et al., 2016). As a result, the PPCC sample visually had a more similar microbial profile at the genus level to other dental calculus samples than the PPL samples (Figure 4).

The MetaPhlAn pipeline was used to corroborate the metagenomic communities characterized by QIIME. MetaPhlAn failed to identify Chloroflexi and TM7 in the Teotihuacan samples but was able to identify the other eight phyla (Figure 5). MetaPhlAn also showed that the PPCC sample had a different microbial profile from the PPL samples at the genus level (Figure 6). The species-level analysis from MetaPhlAn found several oral taxa in the PPCC sample with a few in the PPL samples (Table 4). MetaPhlAn estimated a high relative abundance of the skin bacterium, *Cutibacterium acnes* (formerly *Propionibacterum acnes*), with a mean of 16.20% in the PPL samples but was less than 0.5% in the PPCC sample (Figure 7).

Microbial Damage Patterns

MapDamage 2.0 was used to authenticate the damage patterns of the microbial DNA from the PPCC and PPL samples using three references: *Methanobrevibacter oralis, S. anginosus,* and *C. acnes*. As a control, inferences were made with only samples that had more than 1000 reads mapped to the references. Only the analysis-ready reads from the PPCC, PPL 5A, and PPL 5B samples show damage patterns at the 5' and 3' termini inserts expected for aDNA when mapped to the *M. oralis* (Figure 8). The reads from the PPCC and PPL 5A samples show damage when mapped to *S. anginosus* (Figure 9). None of the reads from the Teotihuacan samples show damage when mapped to *C. acnes* (Figure 10).

Microbial fragment length analysis

Based on the metataxonomic results, reads from each sample was mapped to three bacteria: *M. oralis, S. anginosus* and *C. acnes*. The median fragment length for the PPCC sample when mapped to *M. oralis* (93 bp) and *S. anginosus* (72 bp) were longer than the median for *C.*

acnes (44 bp) (Table 5). The PPL samples, on the other hand, had longer median fragment lengths when mapped to the human reference in comparison to the bacteria references. In addition, the fragmentation length distributions were also visualized in R. Fragmentation length distribution for aDNA generally have medians that are less than 100 bps (Kistler et al., 2017). This pattern was observed across all samples. However, the median for fragment lengths from the PPCC sample was longer than the median for the PPL samples when mapped to *M. oralis* (Figure 11). A similar pattern was also observed for the PPCC and PPL 5A sample when mapped to *S. anginosus* (Figure 12). This pattern could also be observed when the reads for the Teotihuacan samples were mapped to *C. acnes* (Figure 13). However, the damage patterns for each sample suggest that all *C. acnes* reads were modern contaminants.

Bayesian source tracking

SourceTracker was performed to estimate the environmental origin of the microbial DNA present within each sample based on a set of modern well-characterized reference communities sequenced from human dental calculus (Mann et al., 2018; Weyrich et al., 2017), human gut (Gopalakrishnan et al., 2018; Rampelli et al., 2015), plaque (Lloyd-Price et al., 2017), saliva (Aleti et al., 2018; Lassalle et al., 2018), skin (Oh et al., 2016; Schmedes et al., 2016; Tirosh et al., 2018), and soil (DOE Joint Genome Institute, 2017; Lin et al., 2014) (Figure 13). The oral and skin microbiomes share few taxa members of the genera *Propionibacterium* and *Staphylococcus* which are commonly found in the skin while *Streptococcus* dominates the oral cavity (Mann et al., 2018). Members of the phyla *Acidobacteria* generally dominate soil microbiomes although its relative abundance is highly variable (Lee et al., 2008). Only the PPCC sample visually showed a strong dental calculus signal (97% attributable to dental calculus), whereas the PPL samples showed a strong soil, skin, and unknown signature than dental calculus (less than 10% attributable to dental calculus for each) (Figure 14). This finding in the PPCC

sample is consistent with the SourceTracker analyses in Mann et al. (2018) and Weyrich et al. (2017) where they used soil, skin, plaque, and unknown as sources. These analyses suggest differential amounts of preservation and contamination between the PPCC and PPL samples.

Human DNA Content

The proportion of human endogenous DNA in dental calculus varies but is generally low (<1.0 %) (Mann et al., 2018). The proportion of human DNA recovered in the Teotihuacan samples is comparable to that found in other samples (Figure 15). However, a concerning issue for this study was that the second extraction blank had more unique reads mapping to hg 19 (87,526) than any of the samples (Table 1).

Mitochondrial haplotypes were characterized for the four samples and the results reveal the presence of H2a2a1 in all samples but this finding is due to the few numbers of reads mapping to the rCRS reference (Table 1). The H2a2a1 is the default haplotype given when there is a lack of complete information. For this reason, no downstream analyses estimating the ancestry of the Teotihuacan samples were made.

Human Damage Patterns and Fragment Lengths

Analysis-ready reads that mapped to the human genome for the PPCC sample visually show damage, whereas the PPL samples do not (Figure 16). This pattern suggests that the human DNA content in the PPL samples are modern contaminants.

The human fragment length distributions for the four Teotihuacan samples were consistent with the microbial fragment length distributions (Figure 17). The median for the human PPCC fragment length distribution (55 bp) was shorter than the medians for *M. oralis* (93 bp) and *S. anginosus* (72 bp). This was not the case for the PPL samples. The median for the

human PPL 5A fragment length distribution (79 bp), PPL 5B (64 bp), and PPL 5C (73 bp) were longer than their respective median fragment length distributions for *M. oralis* and *S. anginosus*.

Table 1. Summary of reads

Sample	Total Reads	Analysis-ready reads	Unique rCRS Reads	Unique hg 19 Reads	Unique M. oralis Reads	Unique S. anginosus Reads	Unique C. acnes Reads
PPCC	12,033,608	11,547,192	2	1,593	1,064,306	44,689	1,318
PPL 5A	10,796,955	10,067,178	38	59,334	612	3,531	6,665
PPL 5B	13,409,888	11,577,133	48	32,770	1,550	10	4,901
PPL 5C	9,974,121	8,929,205	16	9,449	71	4	3,184
Teo.ExtNeg.1	11,014,302	10,261,598	10	6,970	115	7	1.447
Teo.ExtNeg.2	11,856,703	11,011,285	40	87,526	62	8	878
Teo.LibNeg	408,363	12,007	-	0	-	0	14

Table 2. Relative abundances for known oral bacterial phyla* from QIIME (Q) and MetaPhlAn (MP) within the samples

Taxa	PPCC MP	PPCC Q	PPL 5A MP	PPL 5A Q	PPL 5B MP	PPL 5B Q	PPL 5C MP	PPL 5C Q	NegExt.1 MP	Neg Ext. 1 Q	NegExt.2 MP	NegExt.2 Q	Lib Neg MP	LibNeg. Q
Firmicutes	22.5	39.7	47.4	13.2	0.0	5.5	0.0	3.3	0.0	0.0	0.0	0.4	0.0	0.2
Actinobacteria	12.9	23.0	27.9	36.2	45.0	23.6	80.5	33.6	7.0	0.1	42.1	0.1	0.0	0.1
Proteobacteria	5.9	3.2	18.4	35.6	7.7	36.9	19.6	26.8	93.0	0.6	57.9	0.0	0.0	0.1
Bacteroidetes	4.1	2.0	0.0	2.1	0.0	3.0	0.0	1.7	0.0	0.1	0.0	0.1	0.0	0.2
Fusobacteria	0.1	0.4	0.0	0.0	0.0	0.1	0.0	0.0	0.0	0.0	0.0	0.0	0.0	0.1
Euryarchaeota	48.1	12.8	0.0	0.0	0.0	0.2	0.0	0.1	0.0	0.0	0.0	0.0	0.0	0.0
Saccharibacteria	1.5	5.5	0.0	0.4	0.0	0.6	0.0	0.1	0.0	0.0	0.0	0.0	0.0	0.0
Acidobacteria	0.0	0.0	0.0	0.0	0.0	0.1	0.0	0.2	0.0	0.0	0.0	0.0	0.0	0.0

***The taxa presented were at least 0.1% relative abundance in at least one sample, not including the extraction and library blanks.**

Table 3. Relative abundances for bacterial genera* from QIIME and MetaPhlAn within the samples

Taxa	PPCC MP	PPCC Q	PPL 5A MP	PPL 5A Q	PPL 5B MP	PPL 5B Q	PPL 5C Q	PPL 5C MP	Neg Ext.1 MP	NegExt.1 Q	NegExt.2 MP	NegExt.2 Q	Lib Neg MP	Lib Neg Q
Actinomyces	9.7	16.0	16.0	0.9	0.0	0.2	0.6	0.0	6.4	0.0	18.04	0.0	0.0	0.0
Streptococcus	10.0	3.6	1.4	1.3	0.0	0.7	0.1	0.0	0.6	0.0	0.0	0.0	0.0	0.0
Veillonella	0.0	0.0	0.0	0.0	0.0	0.0	0.0	0.0	0.0	0.0	24.1	0.0	0.0	0.0
Methanobrevibacter	48.1	12.0	0.0	0.0	0.0	0.0	0.0	0.0	0.24	0.0	0.0	0.0	0.0	0.0
Prevotella	0.0	0.0	0.0	0.1	0.0	0.3	0.0	0.0	33.5	0.0	0.0	0.0	0.0	0.0
Mogibacteriaceae	0.0	0.1	0.0	0.3	0.0	0.0	0.0	0.0	59.2	0.0	51.0	0.0	0.0	0.0
Fusobacterium	0.1	0.0	0.0	0.0	0.0	0.1	0.0	0.0	0.0	0.0	7.0	0.0	0.0	0.0
Leptotrichia	0.0	0.0	0.0	0.0	0.0	0.0	0.0	0.0	0.0	0.0	0.0	0.0	0.0	0.0
Neisseria	0.0	0.0	0.0	0.1	0.0	0.0	0.1	0.0	0.0	0.0	0.0	0.0	0.0	0.0
Propionibacterium	2.3	0.0	15.2	0.0	7.0	0.0	0.0	26.4	0.0	0.0	0.0	0.0	0.0	0.0

***The taxa presented were at least 0.1% relative abundance in at least one sample, not including the extraction and library blanks.**

Table 4. Relative abundances for bacterial species* from MetaPhlAn

Taxa	PPCC	PPL 5A	PPL 5B	PPL 5C	NegExt.1	NegExt.2	LibNeg
Methanobrevibacter unclassified	48.0	0.0	0.0	0.0	0.0	0.0	0.0
Cutibacterium acnes	2.2	15.1	7.0	26.4	0.6	0.0	0.0
Desulfobulbus sp oral taxon 041	5.6	0.0	0.0	0.0	0.0	0.0	0.0
Bacteroidetes oral taxon_274	0.7	0.0	0.0	0.0	0.0	0.0	0.0
Treponema denticola	0.7	0.0	0.0	0.0	0.0	0.0	0.0
Tannerella forsythia	3.0	0.0	0.0	0.0	0.0	0.0	0.0
Staphylococcus hominis	0.0	28.3	0.0	0.0	0.0	0.0	0.0
Streptococcus anginosus	7.0	16.0	0.0	0.0	0.0	0.0	0.0
Bifobacterium pseudolongum	0.0	0.0	0.0	0.0	0.0	24.1	0.0
Rhodopseudomonas palustris	0.0	0.0	0.0	0.0	0.0	6.9	0.0
Bukholderia spp.	0.0	0.0	0.0	0.0	59.2	51.0	0.0
Polynucleobacter necessaries	0.0	0.0	0.0	0.0	0.2	0.0	0.0
Pseudomonas spp.	0.0	0.0	0.0	0.0	33.6	0.0	0.0

***The top 6 most abundant species within the PPCC sample, top 3 in the PPL 5A, top 1 in the PPL 5B and 5C samples.**

Table 5. Median Fragment Lengths (bp)

	PPCC	PPL 5A	PPL 5B	PPL 5C
Human	55	79	64	73
Methanobrevibacter oralis	93	66	48	50
Streptococcus anginosus	72	64	42.5	59.5
Cutibacterium acnes	44	70	62	61

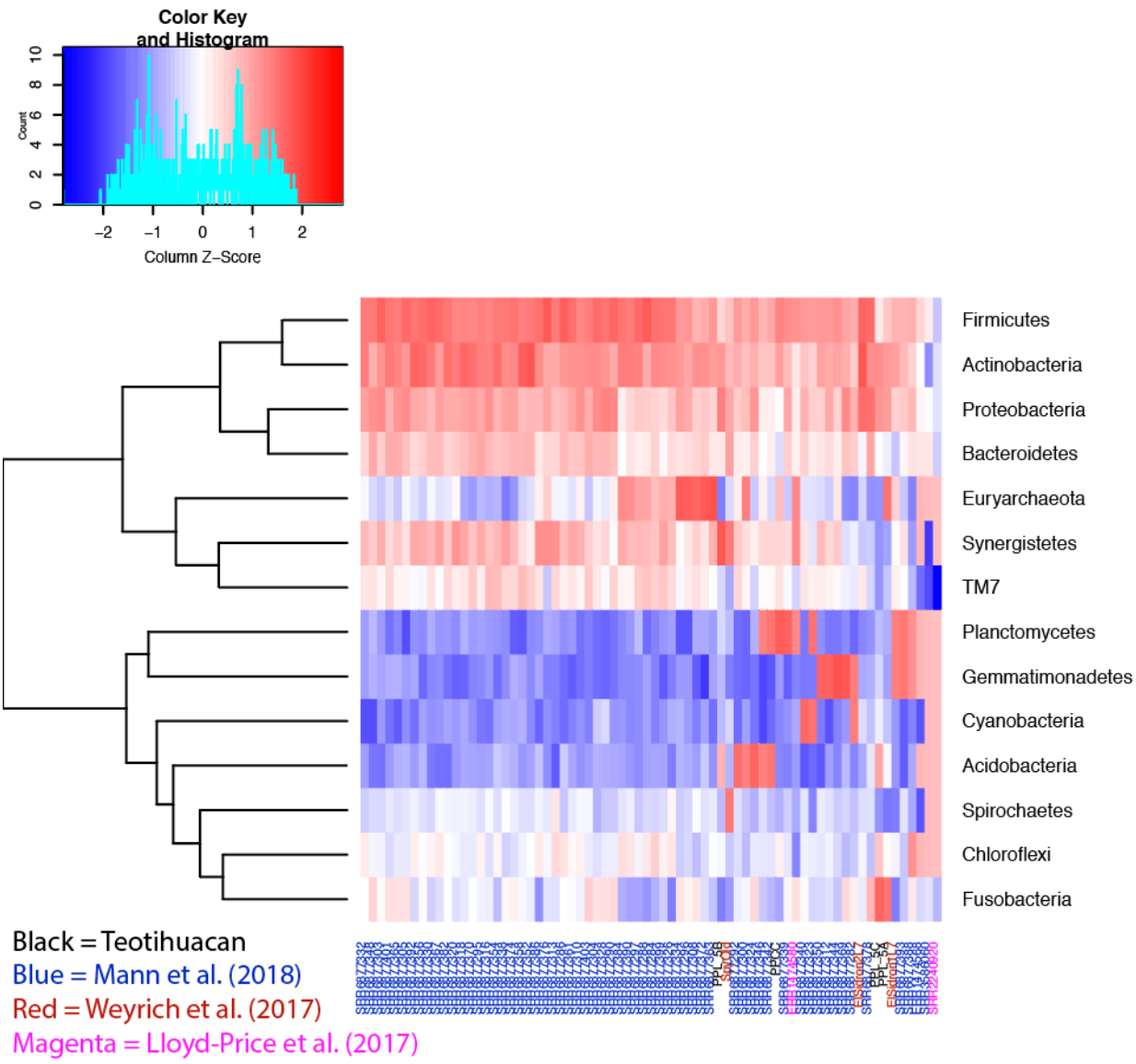

Figure 3. Log transformed relative abundances of phyla identified by QIIME. High abundant taxa are in gradients for red while less abundant taxa are white and blue. The microbial communities depicted are from the Plaza of the Columns sample (PPCC), Moon Pyramid samples (PPL 5A-C, n=3), Neanderthals (n=3, Weyrich et al., 2017), various archaeological contexts (n=59, Mann et al., 2018), and Hunter Gatherers from the Phillipines (n=2, Lassalle et al., 2018). The 14 phyla were present in at least 10% of samples within this study with a relative abundance of at least 0.5%.

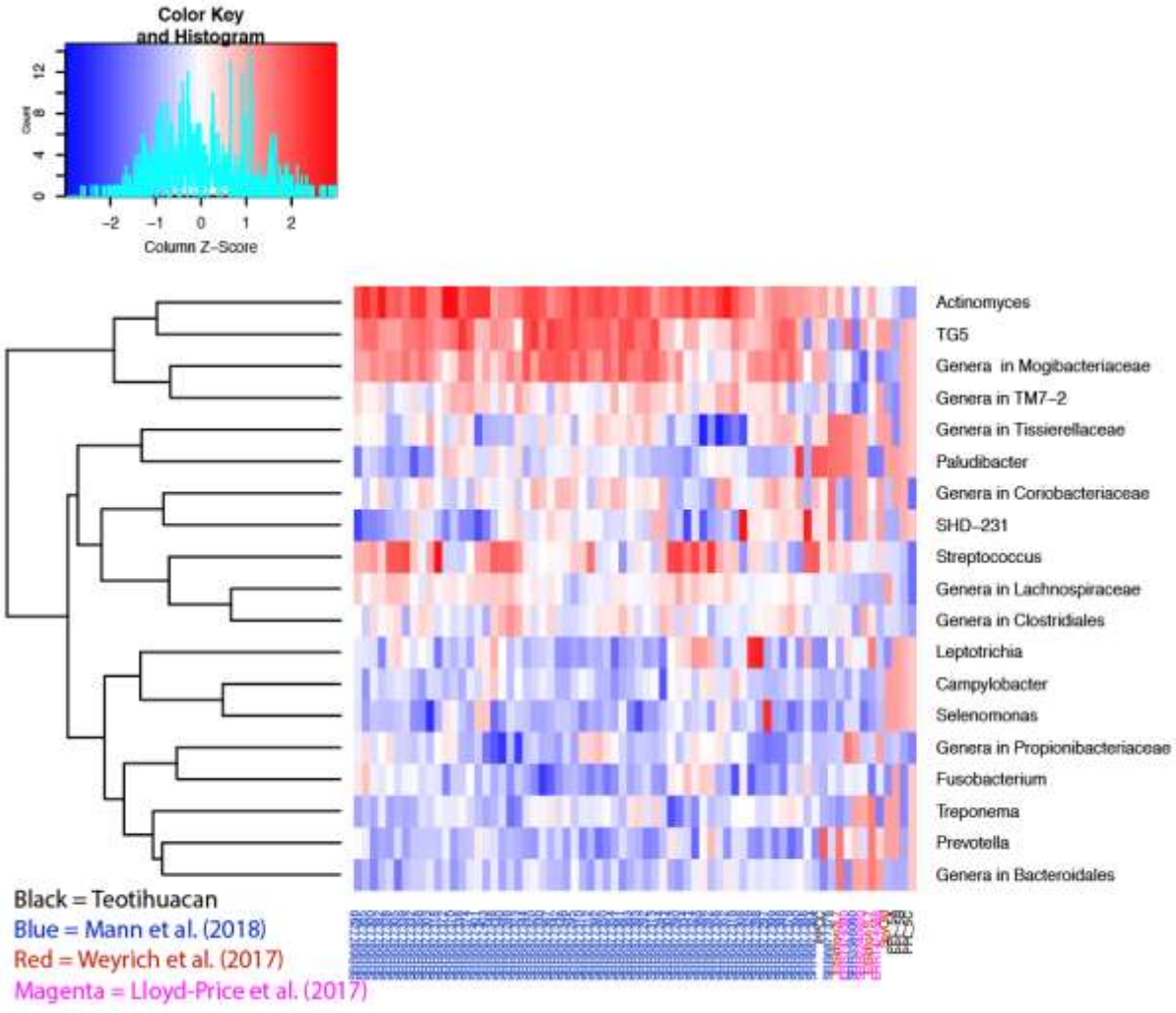

Figure 4. Log transformed relative abundances of genera identified by QIIME. The 19 genera had a relative abundance of at least 0.5% and were present in at least 10% of samples.

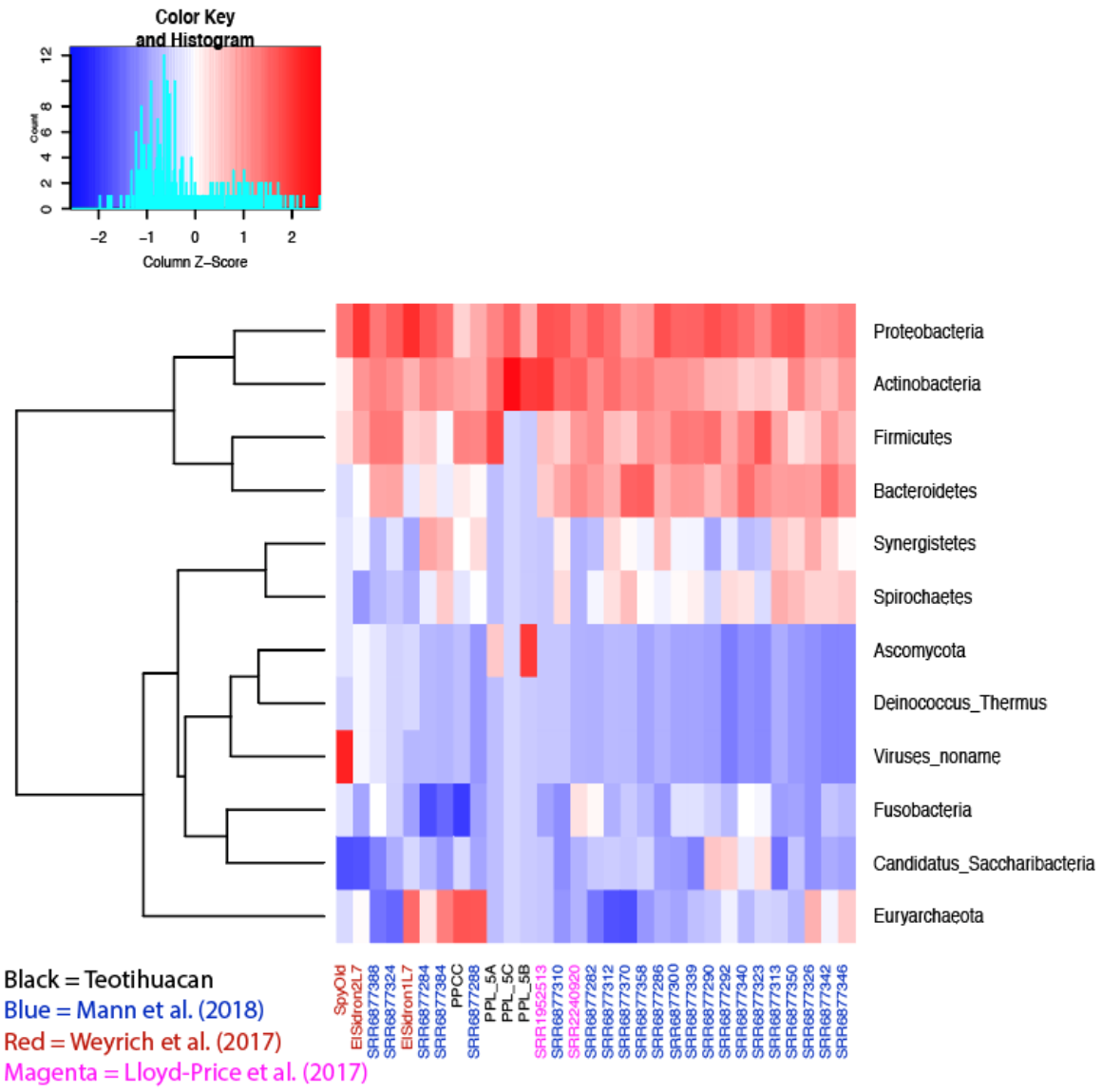

Figure 5. Log transformed relative abundances of phyla identified by MetaPhlAn. The 13 phyla had a relative abundance of at least 0.5% were present in at least 10% of samples.

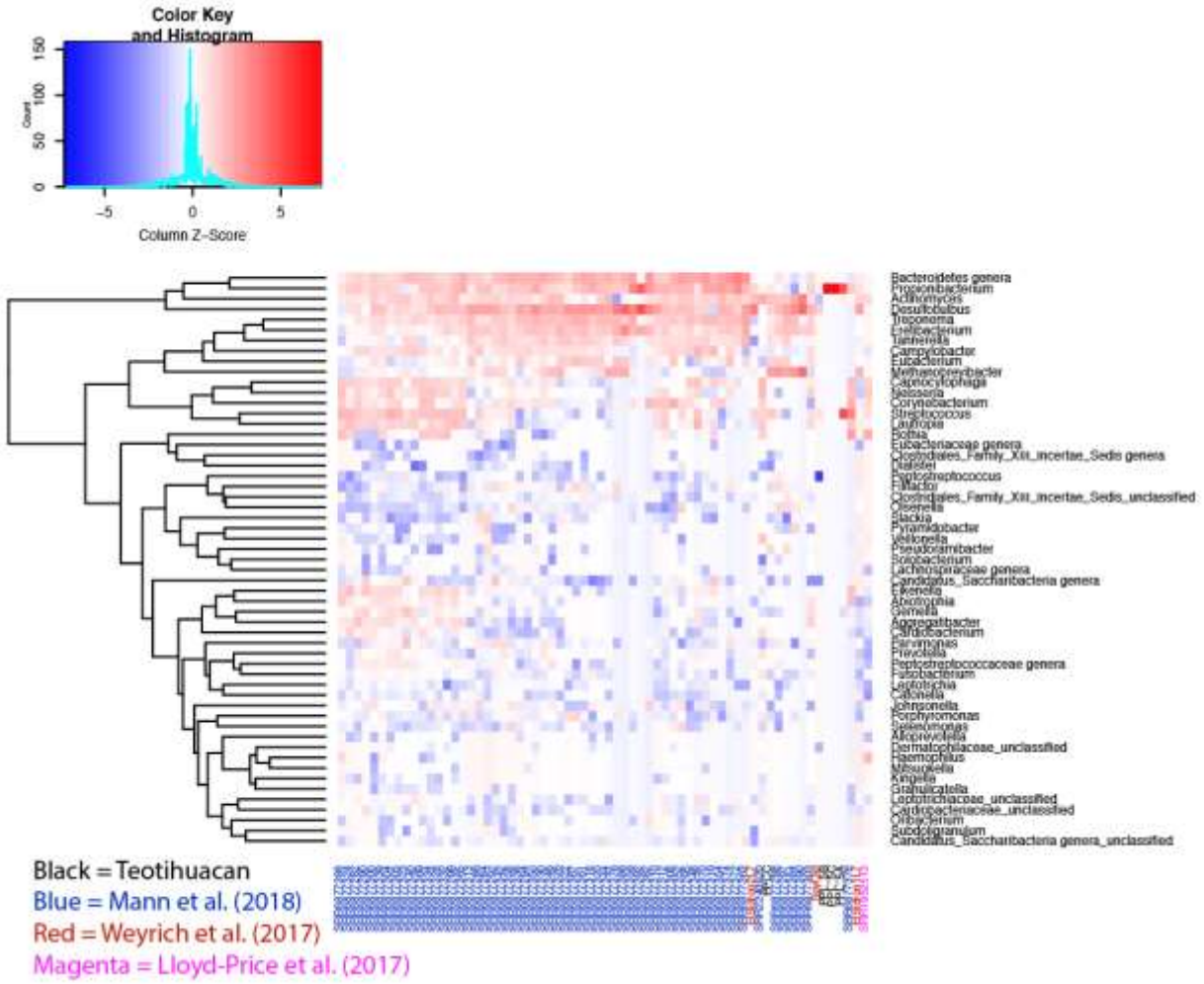

Figure 6. Log transformed relative abundances of genera identified by MetaPhlAn. The 18 genera had at least 0.5% relative abundance and were present in at least 10% of samples. Note that the PPL samples have different microbial profiles with other dental calculus samples. One notable taxon is *Streptococcus anginosus* and its high abundance in the PPL 5A sample. As a result, this taxon *S. anginosus* was used as reference for downstream analyses.

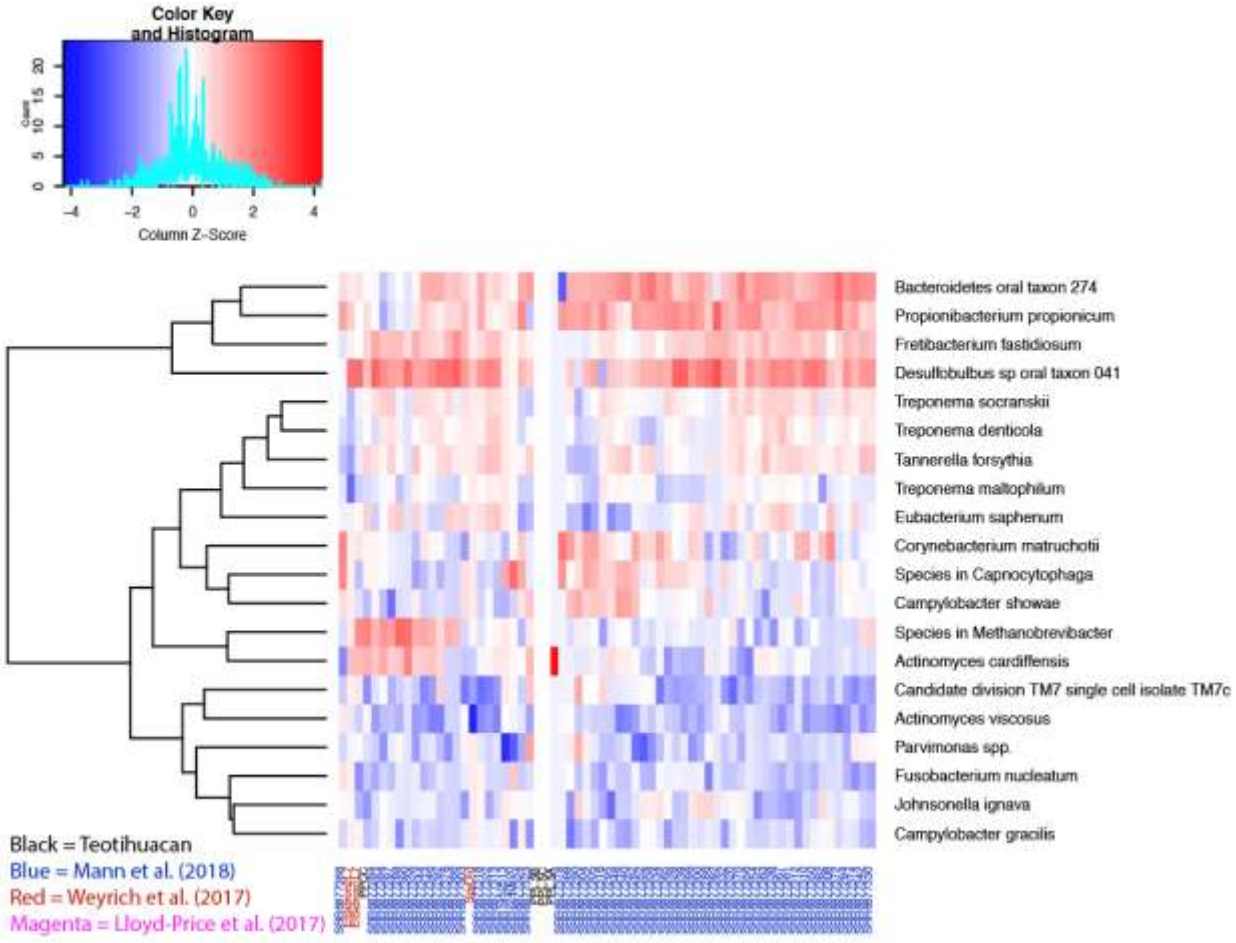

Figure 7. Log transformed relative abundances of species identified by MetaPhlAn. The 20 species had a relative abundance of at least 0.5% and were in at least 10% of samples. Note that the PPL samples have different microbial profiles with other dental calculus samples.

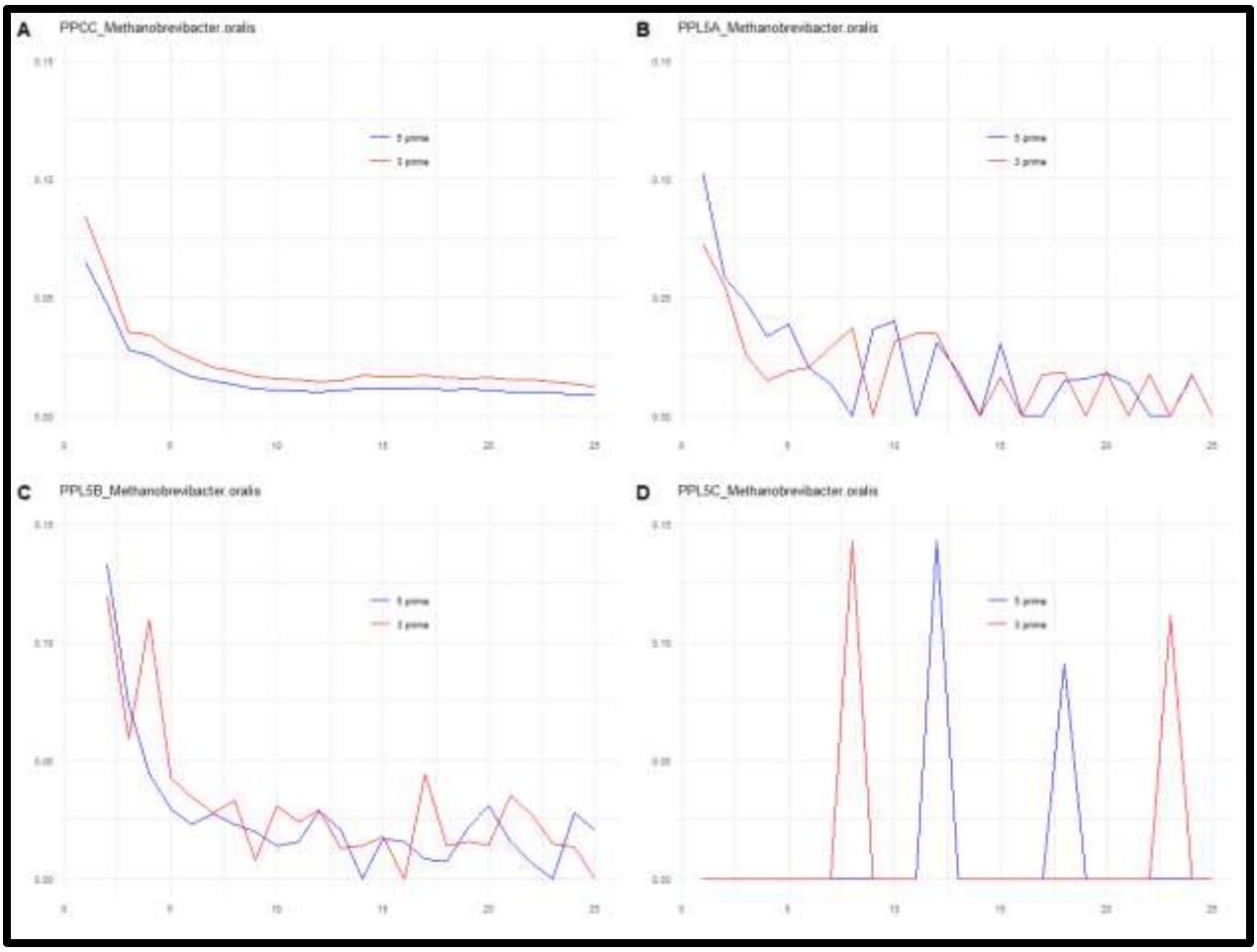

Figure 8. MapDamage results for *M. oralis.* The PPCC, PPL 5A, and PPL 5B samples exhibit expected damage patterns for aDNA, while PPL 5C does not. Unique read counts for each sample: PPCC: 1,064,306; PPL 5A: 612; PPL 5B: 1,550; PPL 5C: 71.

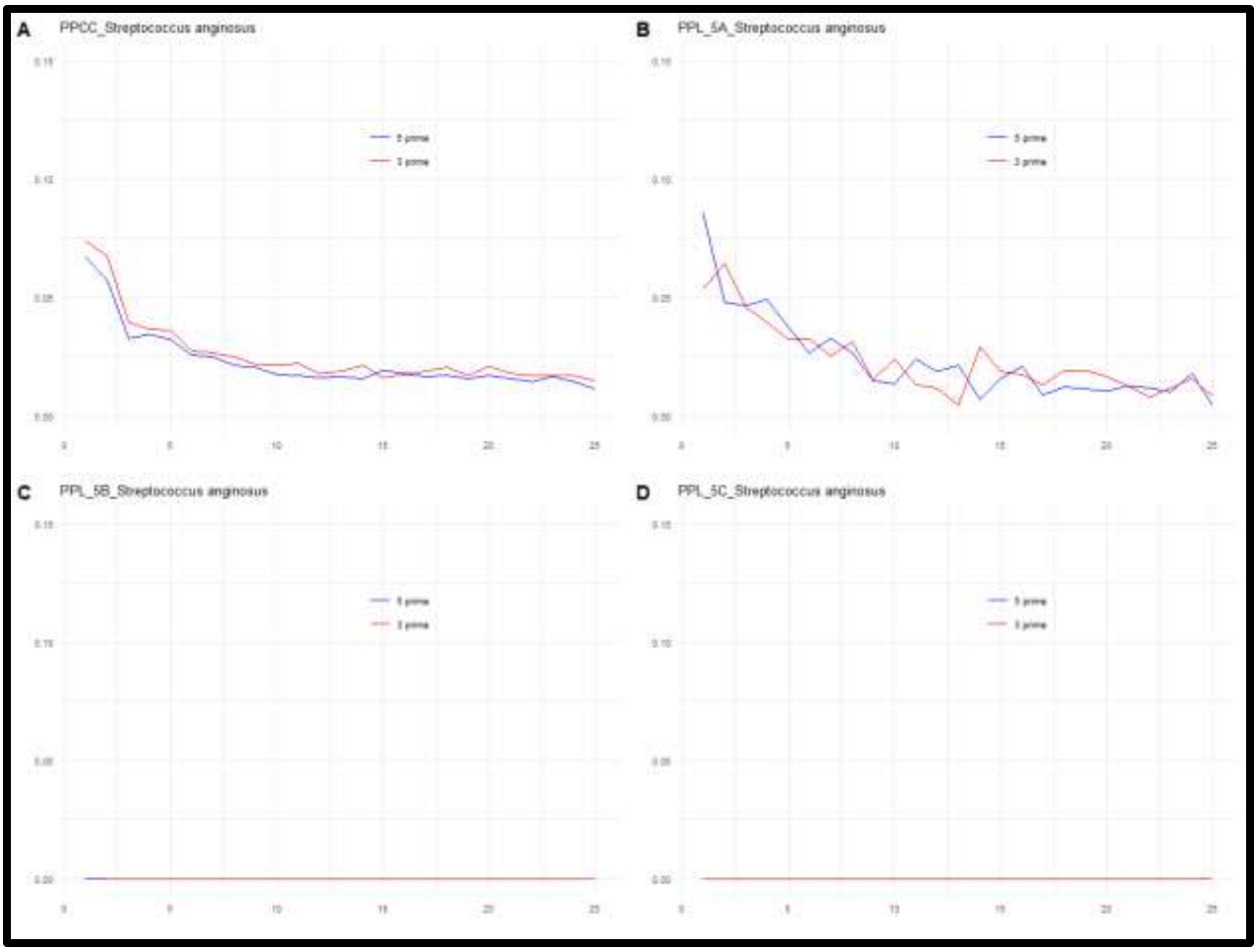

Figure 9. MapDamage results for *S. anginosus*. The PPCC and PPL 5A samples exhibit expected damage patterns for aDNA, while PPL 5B and PPL 5C does not. Unique read counts for each sample: PPCC: 44,689; PPL 5A: 3,531; PPL 5B: 10; PPL 5C: 4.

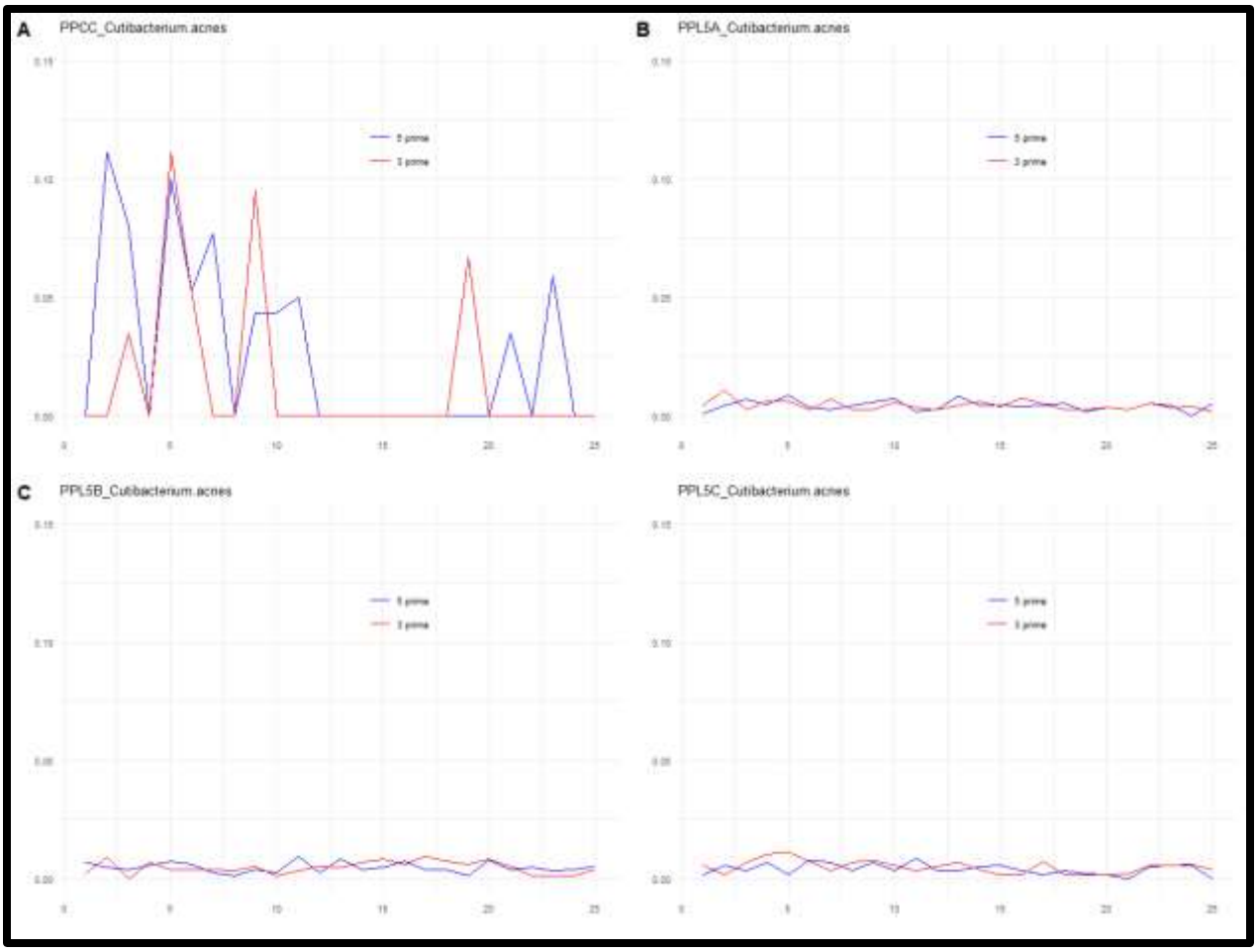

Figure 10. MapDamage results for *C. acnes*. None of the Teotihuacan samples exhibit damage patterns expected for aDNA. Unique read counts for each sample: PPCC: 1,318; PPL 5A: 6,665; PPL 5B: 4,901; PPL 5C: 3,184.

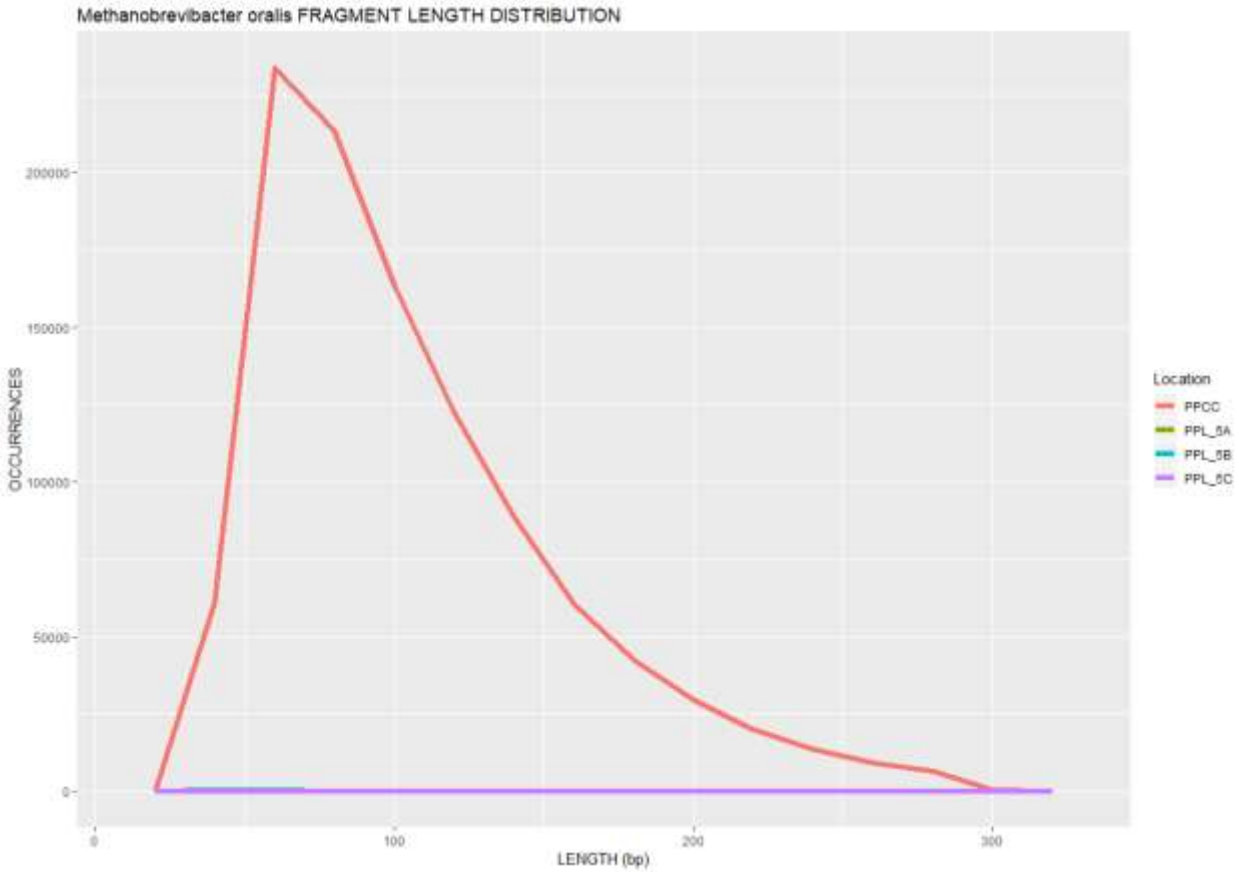

Figure 11. Fragment length distributions for the four samples when mapped to the *M. oralis* reference genome. Note that the PPL samples are also included in this graph but because of their scale, the line appears to be flat. Unique read counts for each sample: PPCC: 1,064,306; PPL 5A: 612; PPL 5B: 1,550; PPL 5C: 71.

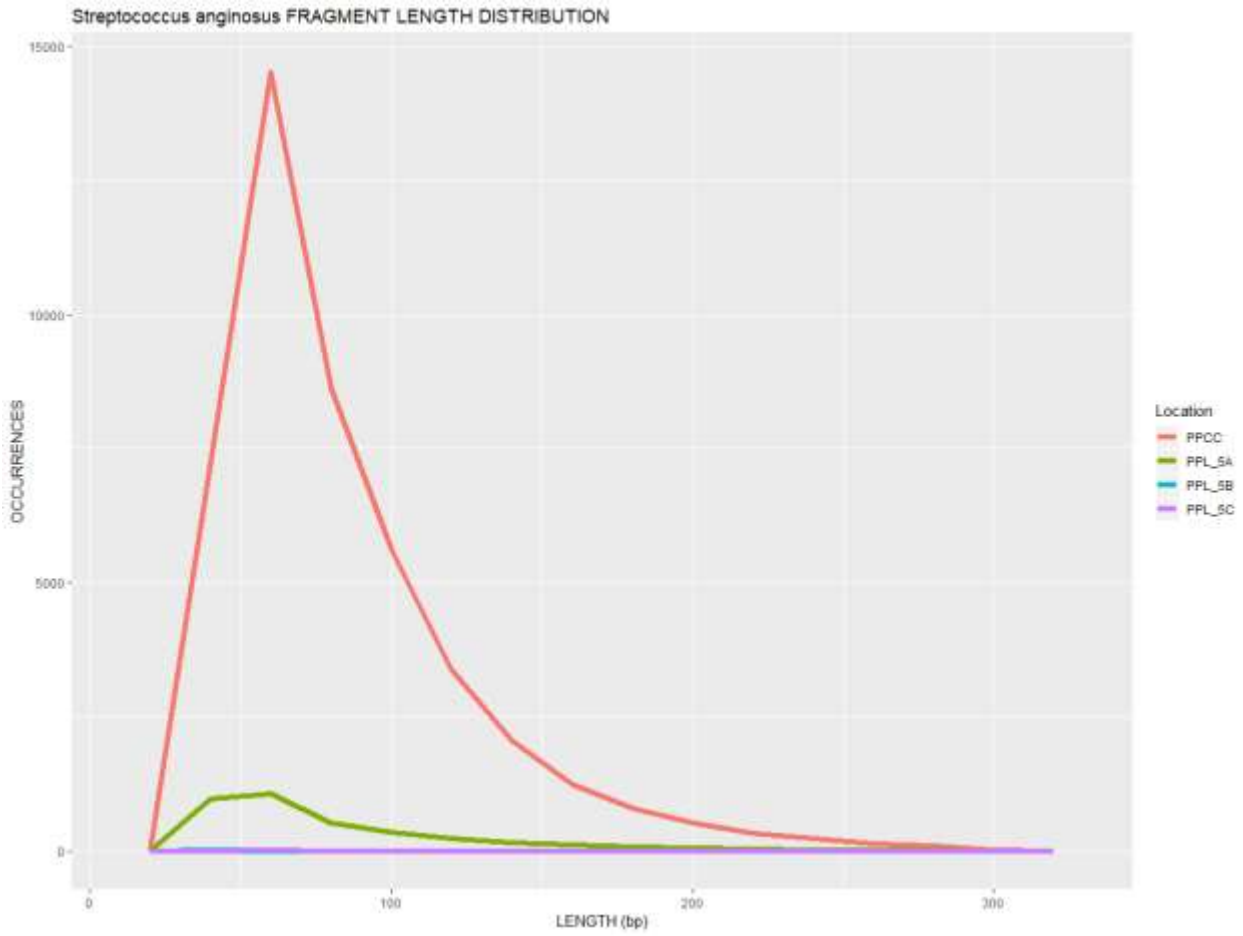

Figure 12. Fragment length distributions for the four samples when mapped to the *S. anginosus* reference genome. Note that the PPL 5B sample is also included in this graph but because of their scale, their lines appear to be flat. Unique read counts for each sample: PPCC: 44,689; PPL 5A: 3,531; PPL 5B: 10; PPL 5C: 4.

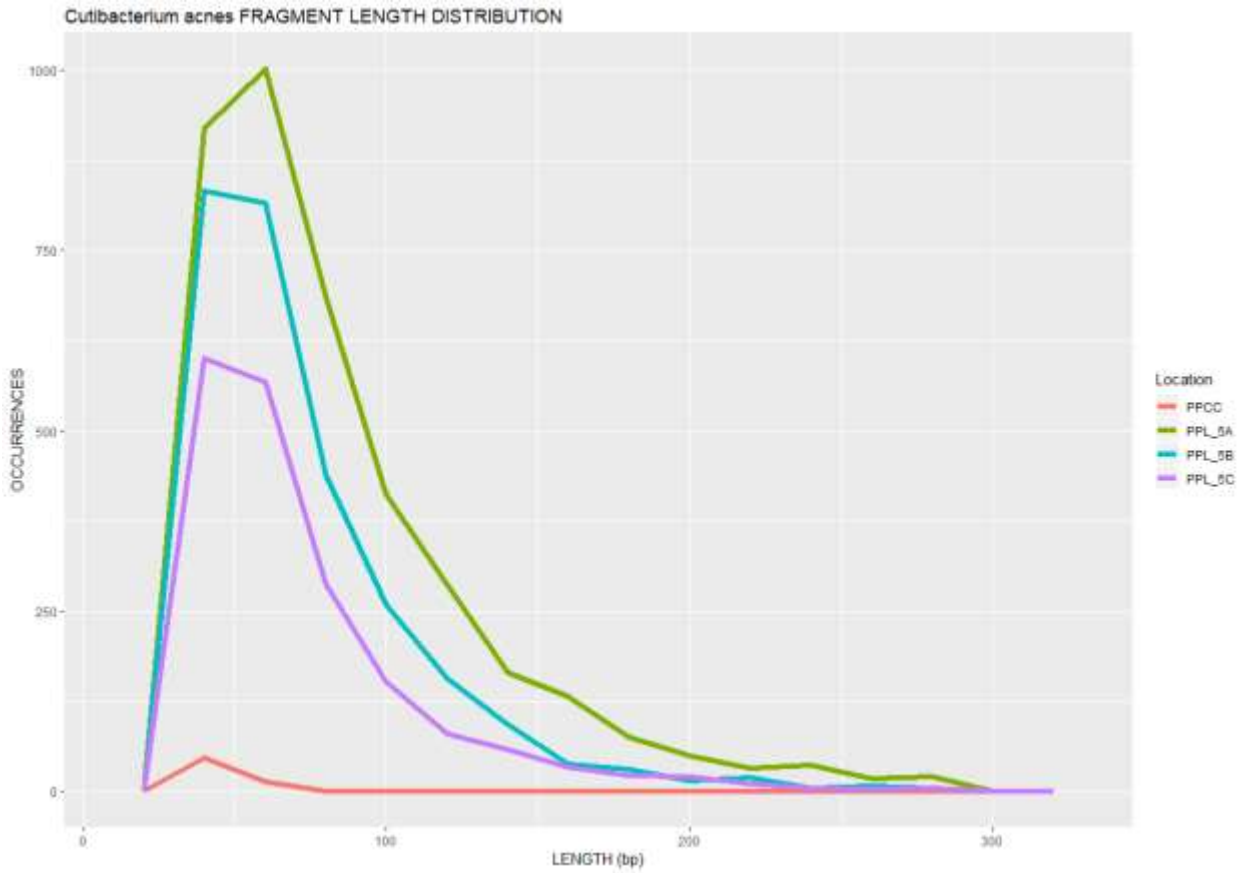

Figure 13. Fragment length distributions for the four samples when mapped to *C. acnes*. Note that the PPCC had few DNA sequences mapped to *C. acnes* while the PPL samples had more than 500. Unique read counts for each sample: PPCC: 1,318; PPL 5A: 6,665; PPL 5B: 4,901; PPL 5C: 3,184.

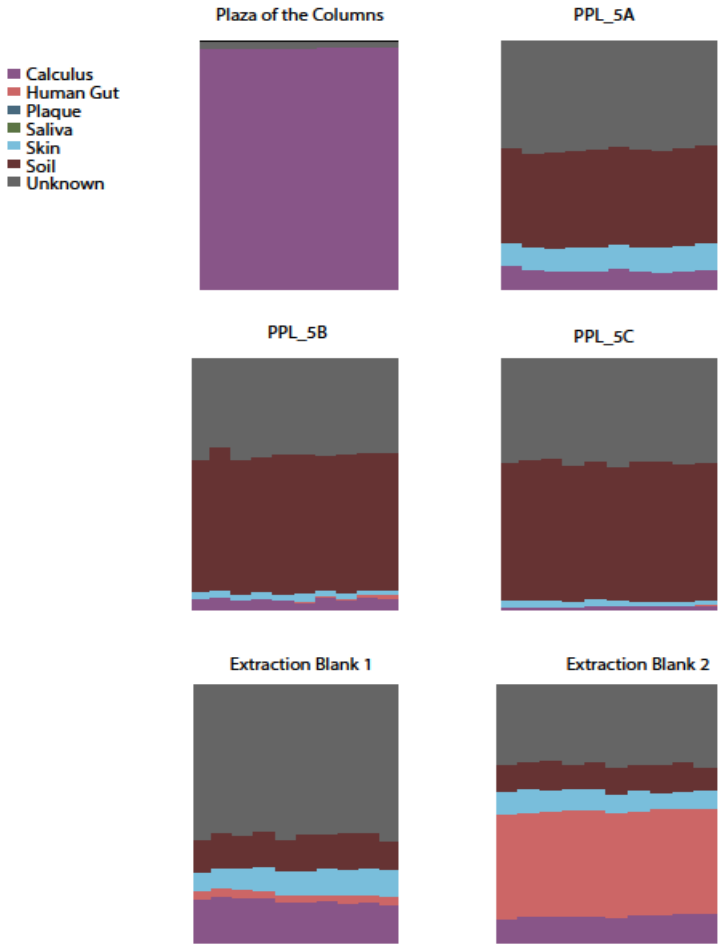

Figure 14. Bayesian source-tracking results at the genus-level for ancient dental calculus and extraction blank samples. The PPCC sample almost entirely assigns to dental calculus sources from Neanderthals (Weyrich et al., 2017) and a global dental calculus dataset (Mann et al., 2018). The PPL samples assign partially to skin sources (DOE Joint Genome Institute, 2017).

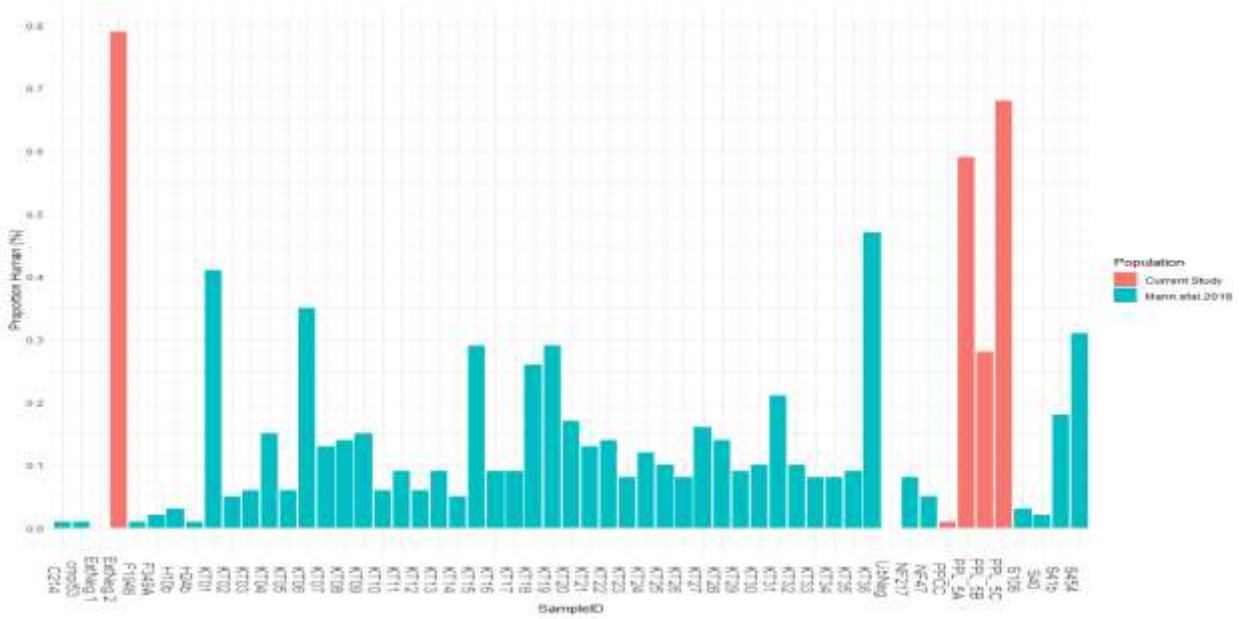

Figure 15. Percent of human endogenous content among dental calculus samples. The data has been transformed. The four Teotihuacan samples are highlighted in teal while the dental calculus samples from Mann et al. (2018) are depicted in salmon. Note that the ExtNeg.2 sample has a much higher proportion of human reads than any other sample included in this study. The PPL 5B and PPL 5C also had a considerable proportion of human DNA, which has not yet been demonstrated in previous calculus studies. While standard precautions to minimize contamination were observed, human contamination seems to be an issue.

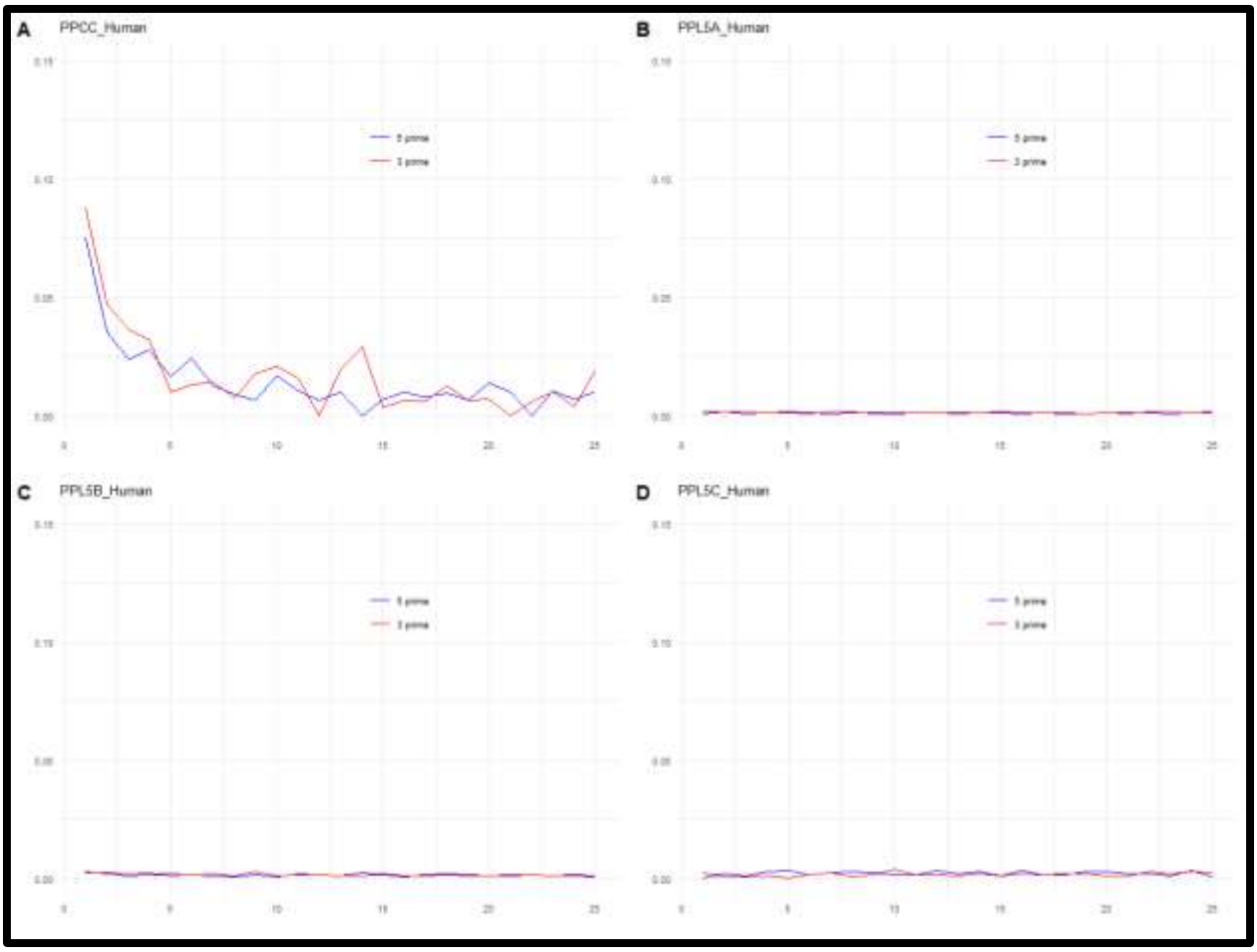

Figure 16. MapDamage results for the human genome. The PPCC exhibit expected damage patterns for aDNA, while PPL 5A, PPL 5B and PPL 5C do not. Unique read counts for each sample: PPCC: 1,593; PPL 5A: 59,334; PPL 5B: 32,770; PPL 5C 9,449.

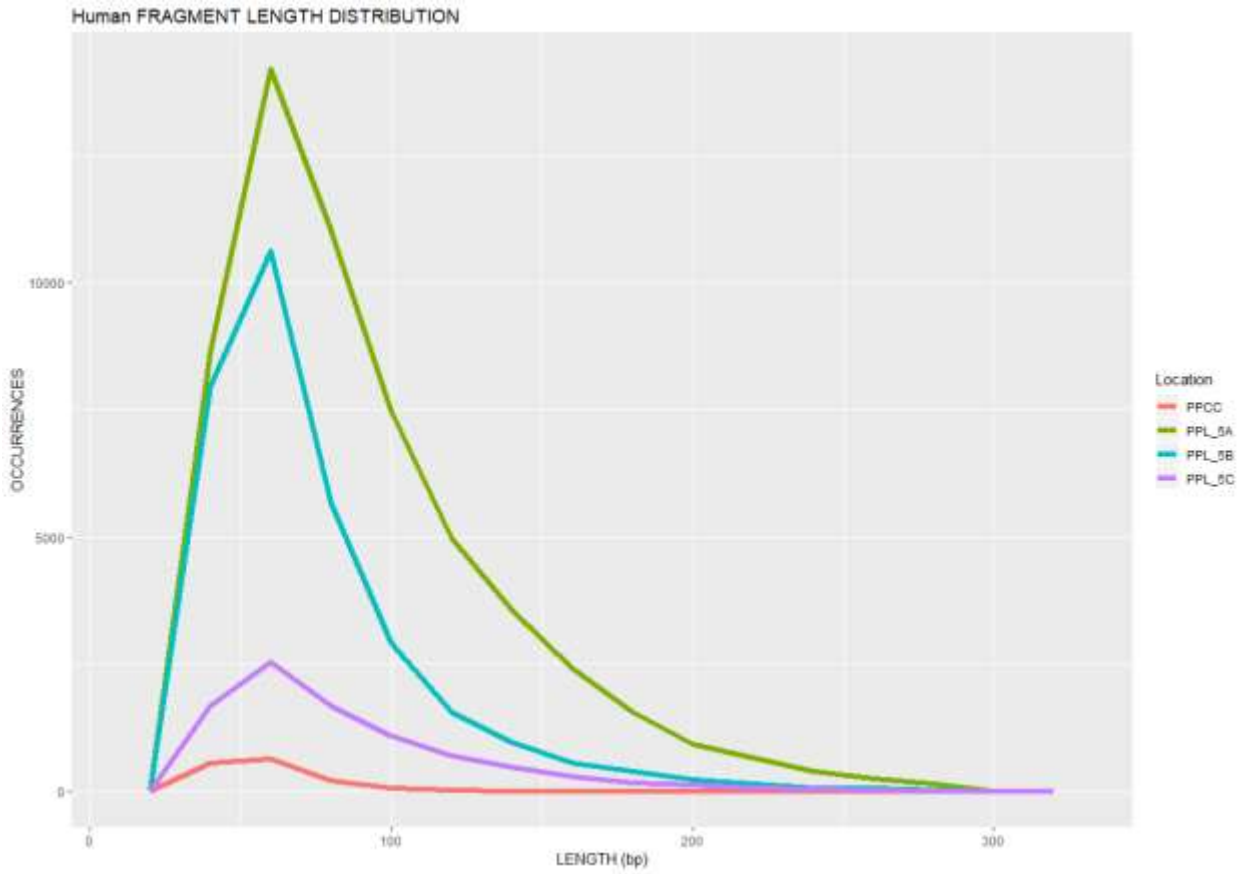

Figure 17. Fragment length distributions for the four samples when mapped to the human reference genome. Unique read counts for each sample: PPCC: 1,593; PPL 5A: 59,334; PPL 5B: 32,770; PPL 5C 9,449. Although these patterns are consistent with previous aDNA samples, their damage patterns indicate that they are modern contaminants (Figure 16).

Discussion

An initial aim of this study was to determine whether it was possible to estimate genetic ancestry from Mesoamerican dental calculus samples. The results presented here were unable to recover a sufficient amount of data to address this question. Nevertheless, this study was able to provide empirical data about DNA preservation of dental calculus in Mesoamerica, an archaeological context unrepresented in previous dental calculus studies (Mann et al., 2018; Warinner et al., 2014; Weyrich et al., 2017). Using several different approaches, we found that the preservation and contamination of microbial and human DNA in dental calculus differs between the samples from the Moon Pyramid and the Plaza of the Columns Complex.

Identification of oral, skin, and soil microbes in the Teotihuacan samples

As a result of the rapid development of software for metataxonomic classification, two different programs were utilized in this study—QIIME and MetaPhlAn. Both programs have been tested *in silico* mock communities with typical aDNA patterns and each has been shown to have advantages and disadvantages in profiling microbial communities (Velsko et al., 2018). For instance, MetaPhlAn underestimates the presence of Chloroflexi within a sample in comparison to other pipelines based on results from mock communities (Lindner and Renard, 2015). MetaPhlAn also has far fewer number of references (~17,000) in comparison to QIIME (~1,000,000). However, the database of MetaPhlAn enables the identification of several species since it uses specific clade markers to identify taxa. Thus, each program is susceptible to false positive and false negatives and applying more than one method is needed to verify results.

In the Teotihuacan samples, both programs identified similar taxa at the phylum- and genus- level in all four samples—oral taxa for the PPCC sample and soil and skin taxa for the PPL samples. Previous research has suggested that 16S rRNA gene sequencing is more reliable in identification of genera (>90%) rather than in species (65 to 83%) (Janda and Abbott, 2007).

For this reason, only MetaPhlAn was used to identify species in the dental calculus samples. In the PPCC sample, MetaPhlAn identified several oral species, including *Tannerella forsythia*, *Methanobrevibacter spp.*, and *Desulfobulbus* oral taxon 041 (Figure 13). It is well known that both *T. forsythia* and *M. oralis* have been associated with periodontitis in past and modern populations (Huynh et al., 2015; Warinner et al., 2014; Weyrich et al., 2017).

It should be noted that the proportional relative abundance observed in dental calculus is not necessarily reflective of the relative abundance *antemortem*. Nevertheless, in the MetaPhlan analysis, *Methanobrevibacter* was the most abundant organism in the PPCC sample (48.11%). In the QIIME analysis, *Methanobrevibacter* was the second most abundant in the PPCC sample (12.0%) following *Actinomyces* (16.0%). In fact, based on the MetaPhlAn results, the PPCC sample had a higher relative abundance of *Methanobrevibacter* than any sample from Mann et al. (2018) and Weyrich et al. (2017). Furthermore, the only other sample that had *Methanobrevibacter* spp. as the most abundant species was SRR6877288 which is a dental calculus sample from the Caribbean that also dates to prior to European contact. However, only 11% of the reads in the PPCC sample map to the *Methanobrevibacter oralis* reference genome. Mapping the PPCC sample to other *Methanobrevibacter* references may reveal a more accurate estimation of the relative abundance for *Methanobrevibacter* in the sample. Together these data suggest that there are differences between analytical pipelines. More information is needed to determine whether this finding in the two samples is due to a biological process that could be associated with lifestyles in the regions or they are the products taphonomic influences.

The finding of high abundance of *Methanobrevibacter* may come as a surprise. Taxa with lower GC content genomes are more susceptible to denaturation because of their lower melting point (Mann et al., 2018). *Methanobrevibacter* has a low GC content of 27.78%. This

preservation bias for *Methanobrevibacter* may be a result of archaea having different cell wall properties than bacteria (Schleifer, 2009). These properties of archaea are potentially adaptive responses to harsh environments such as permafrost and volcanoes and may explain their robust preservation within dental calculus (Konings et al., 2002; Steven et al., 2009).

The identification of soil taxa (e.g. Acidobacteria representatives), and skin taxa (*Cutibacterium acnes, Staphylococcus hominis,* and *Staphyloccus epidermidis*) in the PPL samples is problematic since their origin remains unclear. However, the curation history for the PPL samples may provide some insight. For instance, these samples have been handled for archaeological, osteological, and isotopic analyses (Spence and Pereira 2007; Sugiyama et al. 2004; Sugiyama et al. 2015). Each analysis exposed the dental calculus enhancing their chances of acquiring contaminants. The samples were treated with UV irradiation in the lab but research has shown that this method as well as HCl treatment fails to completely eliminate contamination (Malmström et al., 2005). The contamination could also have been introduced during the laboratory process, but this is unlikely as the skin and soil taxa identified in the Moon Pyramid samples were not identified in the extraction blanks nor in the PPCC sample (Table 3). The PPCC sample was excavated in 2017, subsampled shortly after excavation, and yielded an oral microbiome signature. For this reason, it is recommended that archaeologists who are considering genetic analyses on dental calculus consider subsampling shortly after the materials have been unearthed.

Authentication of the microbial sequences

The microbial DNA obtained from the PPCC and PPL dental calculus samples derives from distinct communities (i.e. calculus, soil and skin) (Figure 14). In the past, dental calculus studies used SourceTracker to predict the proportion of the community attributable to dental

plaque within a dental calculus sample (Mann et al., 2018; Warinner et al., 2014). Since the rapid accumulation of ancient dental calculus sequence data, this current study is unique in that it used source data from dental calculus (Mann et al., 2018; Weyrich et al., 2017), plaque (Lloyd-Price et al., 2017), and saliva (Aleti et al., 2018; Lassalle et al., 2018) as sources. The SourceTracker analysis predicted 97.4% of the PPCC community could be attributed to dental calculus (Mann et al., 2018; Weyrich et al., 2017). By contrast, microbial DNA within the PPL samples is predicted to be from soil ($\overline{X}$ =48.38%) and bacteria from unknown sources ($\overline{X}$ = 41.2%), with minor contributions from dental calculus. Thus, the findings of this study differs from previous studies in that dental calculus was generally dominated by human-associated oral taxa (Mann et al., 2018; Warinner et al., 2015, 2014). The state of DNA preservation found in the PPL samples may also suggest that dental calculus may not retain a robust oral microbial signature.

Since the PPL samples were excavated at the same archaeological site and date to the same time period as the PPCC sample, it is unlikely that geography has had a significant effect on the DNA preservation of dental calculus. Burial environment might have had some influence on the differential preservation between the PPCC and PPL samples but more sampling from the Plaza of the Columns Complex as well as other Mesoamerican contexts are needed in order to determine whether the patterns observed for PPL samples are typical.

Human DNA recovered from the Teotihuacan samples

Previous studies have demonstrated that the amount of human DNA preserved in dental calculus varies but is generally less than one percent (Mann et al., 2018; Ozga et al., 2016) (Figure 15). This pattern was also observed in this study as the proportion of human DNA was low across all calculus samples (<1.0%). Dental calculus can yield enough authentic host DNA to estimate ancestry when using enrichment processes such as sequence capture (Ozga et al.,

2016; Ziesemer et al., 2019). While sequence capture may be useful in identifying the ancestry of the PPCC sample, it may not be appropriate for the PPL samples as the human DNA in the PPL samples are likely modern contaminants. The PPL samples do not show the expected pattern of C→T substitutions at the 5' ends and the lack of G→A substitutions on the 3' ends (Figure 16). Although the PPCC sample exhibited aDNA damage and fragments with median lengths of 55 bp, there was not enough coverage (<0.001) to accurately estimate mitochondrial ancestry using HaploGrep. However, further analyses could potentially estimate ancestry.

Shotgun sequencing of dental calculus may still be useful in determining whether the human DNA within dental calculus is from the host or the result of contamination. For instance, Mann et al. (2018) found that human DNA fragments are generally shorter than microbial DNA fragments. This pattern was observed in the PPCC sample but not in the PPL samples (Table 5). This difference as well as the results from MapDamage and SourceTracker strongly suggests differential preservation of human and microbial DNA in the dental calculus from the PPL samples in comparison to other dental calculus samples. If the percent of human DNA is higher than 1% in calculus, and does not exhibit the expected damage patterns for aDNA, then the human DNA obtained from the dental calculus is likely from modern contaminants. Moreover, the application of other bioinformatic tools, such as Contamix, could also provide estimations of contamination (Schubert et al., 2014).

The process of human DNA being entrapped into the dental calculus matrix *antemortem* is still poorly understood (Mann et al., 2018). However, the process of contaminant DNA incorporated into the matrix for sequencing is understood even less. Human contaminants in the PPL samples are not likely host but modern contaminants because they did not exhibit aDNA damage despite their fragmentation patterns. The PPCC sample, on the other hand, exhibit both

aDNA damage and the expected short DNA fragment lengths. The patterns observed in the PPL samples have not been observed in previous dental calculus studies (Mann et al., 2018; Warinner et al., 2014; Weyrich et al., 2017). Although the samples in the study were treated with UV irradiation, the application of NaOCl (bleach) to the surface of the calculus could also reduce the amount of contamination recovered (Boessenkool et al., 2017; Kemp and Smith, 2005). Understanding the processes that could have contributed to this differential preservation between the PPL and PPCC could be quite useful for future dental calculus research as more scholars request dental calculus samples (Austin et al., 2019).

Conclusion

This study represents a novel step towards assessing the DNA preservation of dental calculus from a Mesoamerican context, a region that has not been included in previous dental calculus studies (Mann et al., 2018; Warinner et al., 2014; Weyrich et al., 2017). The results presented here demonstrate that HTS methods can recover an extant oral microbiome from Teotihuacan, and that the resulting data provide noteworthy insights into the oral microbiome from a pre-European contact population. In contrast, the PPL samples demonstrate that dental calculus can be susceptible to contamination and that the curation history of samples can impact the recovery of biomolecules. While these initial results are promising, a larger sample size from Teotihuacan and Mesoamerica in general will be needed to broaden the understanding of DNA preservation in the region. Identifying the causal agents for this differential preservation and whether they could have been prevented is critical for future analyses.

References

Adler, C.J., Dobney, K., Weyrich, L.S., Kaidonis, J., Walker, A.W., Haak, W., Bradshaw, C.J.A., Townsend, G., Sołtysiak, A., Alt, K.W., Parkhill, J., Cooper, A., 2013. Sequencing ancient calcified dental plaque shows changes in oral microbiota with dietary shifts of the Neolithic and Industrial revolutions. Nat. Genet. 45, 450–455. https://doi.org/10.1038/ng.2536

Aleti, G., Baker, J.L., Tang, X., Alvarez, R., Dinis, M., Tran, N.C., Melnik, A.V., Zhong, C., Ernst, M., Dorrestein, P.C., 2018. Identification of the bacterial biosynthetic gene clusters of the oral microbiome illuminates the unexplored social language of bacteria during health and disease. bioRxiv 431510.

Allentoft, M.E., Sikora, M., Sjögren, K.-G., Rasmussen, S., Rasmussen, M., Stenderup, J., Damgaard, P.B., Schroeder, H., Ahlström, T., Vinner, L., 2015. Population genomics of bronze age Eurasia. Nature 522, 167.

Álvarez-Sandoval, B.A., Manzanilla, L.R., González-Ruiz, M., Malgosa, A., Montiel, R., 2015. Genetic evidence supports the multiethnic character of Teopancazco, a neighborhood center of Teotihuacan, Mexico (AD 200-600). PloS One 10, e0132371.

Anderson, S., Bankier, A.T., Barrell, B.G., Bruijn, M.H.L. de, Coulson, A.R., Drouin, J., Eperon, I.C., Nierlich, D.P., Roe, B.A., Sanger, F., Schreier, P.H., Smith, A.J.H., Staden, R., Young, I.G., 1981. Sequence and organization of the human mitochondrial genome. Nature 290, 457. https://doi.org/10.1038/290457a0

Andrews, R.M., Kubacka, I., Chinnery, P.F., Lightowlers, R.N., Turnbull, D.M., Howell, N., 1999. Reanalysis and revision of the Cambridge reference sequence for human mitochondrial DNA. Nat. Genet. 23, 147. https://doi.org/10.1038/13779

Armitage, P.L., 1975. The extraction and identification of opal phytoliths from the teeth of ungulates. J. Archaeol. Sci. 2, 187–197.

Austin, J.J., Ross, A.J., Smith, A.B., Fortey, R.A., Thomas, R.H., 1997. Problems of reproducibility–does geologically ancient DNA survive in amber–preserved insects? Proc. R. Soc. Lond. B Biol. Sci. 264, 467–474.

Austin, R.M., Sholts, S.B., Williams, L., Kistler, L., Hofman, C.A., 2019. Opinion: To curate the molecular past, museums need a carefully considered set of best practices. Proc. Natl. Acad. Sci. 116, 1471–1474.

Benn, A.M., Heng, N.C., Broadbent, J.M., Thomson, W.M., 2018. Studying the human oral microbiome: challenges and the evolution of solutions. Aust. Dent. J. 63, 14–24.

Boessenkool, S., Hanghøj, K., Nistelberger, H.M., Der Sarkissian, C., Gondek, A.T., Orlando, L., Barrett, J.H., Star, B., 2017. Combining bleach and mild predigestion improves ancient DNA recovery from bones. Mol. Ecol. Resour. 17, 742–751.

Briggs, A.W., Stenzel, U., Johnson, P.L., Green, R.E., Kelso, J., Prüfer, K., Meyer, M., Krause, J., Ronan, M.T., Lachmann, M., 2007. Patterns of damage in genomic DNA sequences from a Neandertal. Proc. Natl. Acad. Sci. 104, 14616–14621.

Brothwell, D.R., 1981. Digging up bones: the excavation, treatment, and study of human skeletal remains. Cornell University Press.

Carballo, D., Sarinana, D.H., Codlin, M., Buckley, G., Hernandez, J.O., 2018. Activity Areas and Political Economy at Teotihuacan's Plaza of the Columns: Investigations in Front E. Presented at the 82nd Annual Meeting of the Society for American Archaeology 2018 Conference, Washington D.C.

Carøe, C., Gopalakrishnan, S., Vinner, L., Mak, S.S.T., Sinding, M.H.S., Samaniego, J.A., Wales, N., Sicheritz-Pontén, T., Gilbert, M.T.P., 2018. Single-tube library preparation for degraded DNA. Methods Ecol. Evol. 9, 410–419. https://doi.org/10.1111/2041-210X.12871

Champlot, S., Berthelot, C., Pruvost, M., Bennett, E.A., Grange, T., Geigl, E.-M., 2010. An Efficient Multistrategy DNA Decontamination Procedure of PCR Reagents for Hypersensitive PCR Applications. PLOS ONE 5, e13042. https://doi.org/10.1371/journal.pone.0013042

Chatters, J.C., Kennett, D.J., Asmerom, Y., Kemp, B.M., Polyak, V., Blank, A.N., Beddows, P.A., Reinhardt, E., Arroyo-Cabrales, J., Bolnick, D.A., 2014. Late Pleistocene human skeleton and mtDNA link Paleoamericans and modern Native Americans. science 344, 750–754.

Chen, Y.E., Fischbach, M.A., Belkaid, Y., 2018. Skin microbiota–host interactions. Nature 553, 427–436. https://doi.org/10.1038/nature25177

Culotta, E., 2015. New life for old bones. Science 349, 358–361. https://doi.org/10.1126/science.349.6246.358

Dabney, J., Knapp, M., Glocke, I., Gansauge, M.-T., Weihmann, A., Nickel, B., Valdiosera, C., García, N., Pääbo, S., Arsuaga, J.-L., Meyer, M., 2013a. Complete mitochondrial genome sequence of a Middle Pleistocene cave bear reconstructed from ultrashort DNA fragments. Proc. Natl. Acad. Sci. 201314445. https://doi.org/10.1073/pnas.1314445110

Dabney, J., Meyer, M., Pääbo, S., 2013b. Ancient DNA damage. Cold Spring Harb. Perspect. Biol. 5, a012567.

Dave, M., Higgins, P.D., Middha, S., Rioux, K.P., 2012. The human gut microbiome: current knowledge, challenges, and future directions. Transl. Res. 160, 246–257.

De La Fuente, C., Flores, S., Moraga, M., 2013. DNA from human ancient bacteria: a novel source of genetic evidence from archaeological dental calculus. Archaeometry 55, 767–778.

DeSantis, T.Z., Hugenholtz, P., Larsen, N., Rojas, M., Brodie, E.L., Keller, K., Huber, T., Dalevi, D., Hu, P., Andersen, G.L., 2006. Greengenes, a chimera-checked 16S rRNA gene database and workbench compatible with ARB. Appl Env. Microbiol 72, 5069–5072.

Dewhirst, F.E., Chen, T., Izard, J., Paster, B.J., Tanner, A.C., Yu, W.-H., Lakshmanan, A., Wade, W.G., 2010. The human oral microbiome. J. Bacteriol. 192, 5002–5017.

Dobney, K., Brothwell, D., 1988. A scanning electron microscope study of archaeological dental calculus, in: Scanning Electron Microscopy in Archaeology. pp. 372–385.

Dobney, K., Brothwell, D., 1986. Dental calculus: its relevance to ancient diet and oral ecology. Teeth Anthropol. 291, 55–81.

DOE Joint Genome Institute, 2017. Bog forest soil microbial communities from Calvert Island, British Columbia, Canada - ECP14_OM3 metagenome.

Eisenhofer, R., Cooper, A., Weyrich, L.S., 2017. Reply to Santiago-Rodriguez et al.: proper authentication of ancient DNA is essential. FEMS Microbiol. Ecol. 93. https://doi.org/10.1093/femsec/fix042

Gao, L., Liu, Y., Kim, D., Li, Y., Hwang, G., Naha, P.C., Cormode, D.P., Koo, H., 2016. Nanocatalysts promote Streptococcus mutans biofilm matrix degradation and enhance bacterial killing to suppress dental caries in vivo. Biomaterials 101, 272–284.

Gilbert, M.T.P., Bandelt, H.-J., Hofreiter, M., Barnes, I., 2005. Assessing ancient DNA studies. Trends Ecol. Evol. 20, 541–544.

Ginolhac, A., Rasmussen, M., Gilbert, M.T.P., Willerslev, E., Orlando, L., 2011. mapDamage: testing for damage patterns in ancient DNA sequences. Bioinformatics 27, 2153–2155. https://doi.org/10.1093/bioinformatics/btr347

Giongo, A., Gano, K.A., Crabb, D.B., Mukherjee, N., Novelo, L.L., Casella, G., Drew, J.C., Ilonen, J., Knip, M., Hyöty, H., 2011. Toward defining the autoimmune microbiome for type 1 diabetes. ISME J. 5, 82.

Golenberg, E.M., Giannasi, D.E., Clegg, M.T., Smiley, C.J., Durbin, M., Henderson, D., Zurawski, G., 1990. Chloroplast DNA sequence from a Miocene Magnolia species. Nature 344, 656. https://doi.org/10.1038/344656a0

Gomez-Arango, L.F., Barrett, H.L., McIntyre, H.D., Callaway, L.K., Morrison, M., Nitert, M.D., 2016. Connections between the gut microbiome and metabolic hormones in early pregnancy in overweight and obese women. Diabetes 65, 2214–2223.

González-Oliver, A., Márquez-Morfín, L., Jiménez, J.C., Torre-Blanco, A., 2001. Founding amerindian mitochondrial DNA lineages in ancient Maya from Xcaret, Quintana Roo. Am. J. Phys. Anthropol. Off. Publ. Am. Assoc. Phys. Anthropol. 116, 230–235.

Gopalakrishnan, V., Spencer, C.N., Nezi, L., Reuben, A., Andrews, M.C., Karpinets, T.V., Prieto, P.A., Vicente, D., Hoffman, K., Wei, S.C., 2018. Gut microbiome modulates response to anti–PD-1 immunotherapy in melanoma patients. Science 359, 97–103.

Green, R.E., Briggs, A.W., Krause, J., Prüfer, K., Burbano, H.A., Siebauer, M., Lachmann, M., Pääbo, S., 2009. The Neandertal genome and ancient DNA authenticity. EMBO J. 28, 2494–2502.

Hammond, N., Aspinall, A., Feather, S., Hazelden, J., Gazard, T., Agrell, S., 1977. Maya jade: source location and analysis, in: Exchange Systems in Prehistory. Elsevier, pp. 35–67.

Hansen, J.P.H., Medlgaard, J., 1991. Greenland Mummies. McGill-Queen's Press-MQUP.

Hofreiter, M., Paijmans, J.L.A., Goodchild, H., Speller, C.F., Barlow, A., Fortes, G.G., Thomas, J.A., Ludwig, A., Collins, M.J., 2015. The future of ancient DNA: Technical advances and conceptual shifts. BioEssays 37, 284–293. https://doi.org/10.1002/bies.201400160

Hujoel, P., 2009. Dietary carbohydrates and dental-systemic diseases. J. Dent. Res. 88, 490–502.

Huttenhower, C., Gevers, D., Knight, R., Abubucker, S., Badger, J.H., Chinwalla, A.T., Creasy, H.H., Earl, A.M., FitzGerald, M.G., Fulton, R.S., 2012. Structure, function and diversity of the healthy human microbiome. Nature 486, 207.

Huynh, H.T.T., Nkamga, V.D., Drancourt, M., Aboudharam, G., 2015. Genetic variants of dental plaque Methanobrevibacter oralis. Eur. J. Clin. Microbiol. Infect. Dis. 34, 1097–1101. https://doi.org/10.1007/s10096-015-2325-x

Huynh, H.T.T., Verneau, J., Levasseur, A., Drancourt, M., Aboudharam, G., 2016. Bacteria and archaea paleomicrobiology of the dental calculus: a review. Mol. Oral Microbiol. 31, 234–242. https://doi.org/10.1111/omi.12118

International Human Genome Sequencing Consortium, 2001. Initial sequencing and analysis of the human genome. Nature 409, 860–921. https://doi.org/10.1038/35057062

Janda, J.M., Abbott, S.L., 2007. 16S rRNA Gene Sequencing for Bacterial Identification in the Diagnostic Laboratory: Pluses, Perils, and Pitfalls. J. Clin. Microbiol. 45, 2761–2764. https://doi.org/10.1128/JCM.01228-07

Jónsson, H., Ginolhac, A., Schubert, M., Johnson, P.L.F., Orlando, L., 2013. mapDamage2.0: fast approximate Bayesian estimates of ancient DNA damage parameters. Bioinformatics 29, 1682–1684. https://doi.org/10.1093/bioinformatics/btt193

Kemp, B.M., González-Oliver, A., Malhi, R.S., Monroe, C., Schroeder, K.B., McDonough, J., Rhett, G., Resendéz, A., Peñaloza-Espinosa, R.I., Buentello-Malo, L., 2010. Evaluating the farming/language dispersal hypothesis with genetic variation exhibited by populations in the Southwest and Mesoamerica. Proc. Natl. Acad. Sci. 107, 6759–6764.

Kemp, B.M., Smith, D.G., 2005. Use of bleach to eliminate contaminating DNA from the surface of bones and teeth. Forensic Sci. Int. 154, 53–61.

Kirchhoff, P., 1952. Mesoamerica: its geographic limits, ethnic composition and cultural characteristics. Herit. Conqu. 17–30.

Kistler, L., Ware, R., Smith, O., Collins, M., Allaby, R.G., 2017. A new model for ancient DNA decay based on paleogenomic meta-analysis. Nucleic Acids Res. 45, 6310–6320. https://doi.org/10.1093/nar/gkx361

Knapp, M., Clarke, A.C., Horsburgh, K.A., Matisoo-Smith, E.A., 2012. Setting the stage – Building and working in an ancient DNA laboratory. Ann. Anat. - Anat. Anz., Special Issue: Ancient DNA 194, 3–6. https://doi.org/10.1016/j.aanat.2011.03.008

Knights, D., Kuczynski, J., Charlson, E.S., Zaneveld, J., Mozer, M.C., Collman, R.G., Bushman, F.D., Knight, R., Kelley, S.T., 2011. Bayesian community-wide culture-independent microbial source tracking. Nat. Methods 8, 761–763. https://doi.org/10.1038/nmeth.1650

Konings, W.N., Albers, S.-V., Koning, S., Driessen, A.J.M., 2002. The cell membrane plays a crucial role in survival of bacteria and archaea in extreme environments. Antonie Van Leeuwenhoek 81, 61–72. https://doi.org/10.1023/A:1020573408652

Langmead, B., Salzberg, S.L., 2012. Fast gapped-read alignment with Bowtie 2. Nat. Methods 9, 357.

Lassalle, F., Spagnoletti, M., Fumagalli, M., Shaw, L., Dyble, M., Walker, C., Thomas, M.G., Bamberg Migliano, A., Balloux, F., 2018. Oral microbiomes from hunter-gatherers and traditional farmers reveal shifts in commensal balance and pathogen load linked to diet. Mol. Ecol. 27, 182–195.
Lee, S.-H., Ka, J.-O., Cho, J.-C., 2008. Members of the phylum Acidobacteria are dominant and metabolically active in rhizosphere soil. FEMS Microbiol. Lett. 285, 263–269.
Leishman, S.J., Lien Do, H., Ford, P.J., 2010. Cardiovascular disease and the role of oral bacteria. J. Oral Microbiol. 2, 5781.
Lilley, J.M., 1994. The Jewish burial ground at Jewbury. Published for the York Archaeological Trust by the Council for British ….
Lin, X., Tfaily, M.M., Green, S.J., Steinweg, J.M., Chanton, P., Imvittaya, A., Chanton, J.P., Cooper, W., Schadt, C., Kostka, J.E., 2014. Microbial metabolic potential for carbon degradation and nutrient (nitrogen and phosphorus) acquisition in an ombrotrophic peatland. Appl Env. Microbiol 80, 3531–3540.
Lindner, M.S., Renard, B.Y., 2015. Metagenomic profiling of known and unknown microbes with MicrobeGPS. PloS One 10, e0117711.
Linossier, A., Gajardo, M., Olavarria, J., 1996. Paleomicrobiological study in dental calculus: Streptococcus mutans. Scanning Microsc. 10, 1005–13; discussion 1014.
Lloyd-Price, J., Mahurkar, A., Rahnavard, G., Crabtree, J., Orvis, J., Hall, A.B., Brady, A., Creasy, H.H., McCracken, C., Giglio, M.G., McDonald, D., Franzosa, E.A., Knight, R., White, O., Huttenhower, C., 2017. Strains, functions and dynamics in the expanded Human Microbiome Project. Nature 550, 61–66. https://doi.org/10.1038/nature23889
Malmström, H., Storå, J., Dalén, L., Holmlund, G., Götherström, A., 2005. Extensive Human DNA Contamination in Extracts from Ancient Dog Bones and Teeth. Mol. Biol. Evol. 22, 2040–2047. https://doi.org/10.1093/molbev/msi195
Mancl, K.A., Kirsner, R.S., Ajdic, D., 2013. Wound biofilms: lessons learned from oral biofilms. Wound Repair Regen. 21, 352–362.
Mann, A.E., Sabin, S., Ziesemer, K., Vågene, Å.J., Schroeder, H., Ozga, A.T., Sankaranarayanan, K., Hofman, C.A., Fellows Yates, J.A., Salazar-García, D.C., Frohlich, B., Aldenderfer, M., Hoogland, M., Read, C., Milner, G.R., Stone, A.C., Lewis, C.M., Krause, J., Hofman, C., Bos, K.I., Warinner, C., 2018. Differential preservation of endogenous human and microbial DNA in dental calculus and dentin. Sci. Rep. 8. https://doi.org/10.1038/s41598-018-28091-9
Manzanilla, L.R., 2015. Cooperation and tensions in multiethnic corporate societies using Teotihuacan, Central Mexico, as a case study. Proc. Natl. Acad. Sci. 112, 9210–9215.
Marsh, P.D., Martin, M.V., Lewis, M.A., Williams, D., 2009. Oral Microbiology E-Book. Elsevier health sciences.
Mendisco, F., Pemonge, M.H., Leblay, E., Romon, T., Richard, G., Courtaud, P., Deguilloux, M.F., 2015. Where are the Caribs? Ancient DNA from ceramic period human remains in the Lesser Antilles. Phil Trans R Soc B 370, 20130388.
Merriwether, D.A., Reed, D.M., Ferrell, R.E., 1997. Ancient and contemporary mitochondrial DNA variation in the Maya. Bones Maya Stud. Anc. Skelet. 208–217.
Mitchell, D., Willerslev, E., Hansen, A., 2005. Damage and repair of ancient DNA. Mutat. Res. Mol. Mech. Mutagen. 571, 265–276.
Moorhouse, A., Weyrich, L.S., Cooper, A., Gow, N.A.R., Dobney, K., 2015. Identification of Candida spp from ancient DNA extracted from fossilised dental calculus.
Morales-Arce, A.Y., McCafferty, G., Hand, J., Schmill, N., McGrath, K., Speller, C., 2019. Ancient mitochondrial DNA and population dynamics in postclassic Central Mexico: Tlatelolco (ad 1325–1520) and Cholula (ad 900–1350). Archaeol. Anthropol. Sci. https://doi.org/10.1007/s12520-018-00771-7
Morales-Arce, A.Y., Snow, M.H., Kelley, J.H., Anne Katzenberg, M., 2017. Ancient mitochondrial DNA and ancestry of Paquimé inhabitants, Casas Grandes (AD 1200–1450). Am. J. Phys. Anthropol.

Oh, J., Byrd, A.L., Park, M., Kong, H.H., Segre, J.A., Program, N.C.S., 2016. Temporal stability of the human skin microbiome. Cell 165, 854–866.
Ojeda-Garcés, J.C., Oviedo-García, E., Salas, L.A., 2013. Streptococcus mutans and dental caries. Ces Odontol. 26, 44–56.
Okada, M., Soda, Y., Hayashi, F., Doi, T., Suzuki, J., Miura, K., Kozai, K., 2003. Longitudinal study of dental caries incidence with Streptococcus mutans and S-sobrinus in pre-school children., in: JOURNAL OF DENTAL RESEARCH. INT AMER ASSOC DENTAL RESEARCHI ADR/AADR 1619 DUKE ST, ALEXANDRIA, VA 22314-3406 USA, pp. B351–B351.
Ozga, A.T., Nieves-Colón, M.A., Honap, T.P., Sankaranarayanan, K., Hofman, C.A., Milner, G.R., Lewis, C.M., Stone, A.C., Warinner, C., 2016. Successful enrichment and recovery of whole mitochondrial genomes from ancient human dental calculus. Am. J. Phys. Anthropol. 160, 220–228. https://doi.org/10.1002/ajpa.22960
Pääbo, S., 1985. Preservation of DNA in ancient Egyptian mummies. J. Archaeol. Sci. 12, 411–417.
Pääbo, S., Poinar, H., Serre, D., Jaenicke-Després, V., Hebler, J., Rohland, N., Kuch, M., Krause, J., Vigilant, L., Hofreiter, M., 2004. Genetic Analyses from Ancient DNA. Annu. Rev. Genet. 38, 645–679. https://doi.org/10.1146/annurev.genet.37.110801.143214
Paranjapye, N., Daggett, V., 2018. De Novo Designed α-Sheet Peptides Inhibit Functional Amyloid Formation of Streptococcus mutans Biofilms. J. Mol. Biol. 430, 3764–3773.
Pereira, G., de Montes, R.I., Carrasco, J.L.E., Parrilla, J.M.G., 2003. Informe sobre la excavación arqueológica de urgencia en el" solar del ayuntamiento" de Las Cabezas de San Juan (Sevilla). Campaña de 2000, in: Anuario Arqueológico de Andalucía 2000. Consejería de Cultura, pp. 1309–1316.
Pereira, G., Spence, M.W., White, C.D., 2004. Análisis preliminar de los restos humanos encontrados en el Entierro 5 de la Pirámide de la Luna, Teotihuacán, in: Society for American Archaeology, 69th Meeting, Montreal.
Poinar, H.N., Cooper, A., 2000. Ancient DNA: do it right or not at all. Science 5482, 416.
Preus, H.R., Marvik, O.J., Selvig, K.A., Bennike, P., 2011. Ancient bacterial DNA (aDNA) in dental calculus from archaeological human remains. J. Archaeol. Sci. 38, 1827–1831.
Price, T.D., Manzanilla, L., Middleton, W.D., 2000. Immigration and the ancient city of Teotihuacan in Mexico: a study using strontium isotope ratios in human bone and teeth. J. Archaeol. Sci. 27, 903–913.
Raff, J.A., Bolnick, D.A., Tackney, J., O'Rourke, D.H., 2011. Ancient DNA perspectives on American colonization and population history. Am. J. Phys. Anthropol. 146, 503–514.
Rampelli, S., Schnorr, S.L., Consolandi, C., Turroni, S., Severgnini, M., Peano, C., Brigidi, P., Crittenden, A.N., Henry, A.G., Candela, M., 2015. Metagenome sequencing of the Hadza hunter-gatherer gut microbiota. Curr. Biol. 25, 1682–1693.
Rasmussen, S., Allentoft, M., Nielsen, K., Orlando, L., Sikora, M., Pedersen, A., Schubert, M., VanáDam, A., Kapel, C., Avetisyan, P., 2015. Early divergent strains of Yersinia pestis in Eurasia 5,000 years ago. Cell 163, 571–582.
Robb, M., 2017. Teotihuacan: City of Water, City of Fire. Univ of California Press.
Rohland, N., Reich, D., 2012. Cost-effective, high-throughput DNA sequencing libraries for multiplexed target capture. Genome Res. 22, 939–946.
Rowles, S., 1961. Further studies on the crystalline constituents of oral calculus. J Dent Res 40, 1284.
Salter, S.J., Cox, M.J., Turek, E.M., Calus, S.T., Cookson, W.O., Moffatt, M.F., Turner, P., Parkhill, J., Loman, N.J., Walker, A.W., 2014. Reagent and laboratory contamination can critically impact sequence-based microbiome analyses. BMC Biol. 12, 87. https://doi.org/10.1186/s12915-014-0087-z
Santiago-Rodriguez, T.M., Fornaciari, G., Luciani, S., Dowd, S.E., Toranzos, G.A., Marota, I., Cano, R.J., 2016. Taxonomic and predicted metabolic profiles of the human gut microbiome in pre-Columbian mummies. FEMS Microbiol. Ecol. 92, fiw182.

Sawafuji, R., Saso, A., Suda, W., Hattori, M., Ueda, S., 2018. Ancient DNA analysis of food remains in human dental calculus from the Edo period, Japan. bioRxiv 246868. https://doi.org/10.1101/246868
Sawyer, S., Krause, J., Guschanski, K., Savolainen, V., Pääbo, S., 2012. Temporal Patterns of Nucleotide Misincorporations and DNA Fragmentation in Ancient DNA. PLOS ONE 7, e34131. https://doi.org/10.1371/journal.pone.0034131
Schleifer, K.H., 2009. Classification of Bacteria and Archaea: Past, present and future. Syst. Appl. Microbiol. 32, 533–542. https://doi.org/10.1016/j.syapm.2009.09.002
Schmedes, S.E., Sajantila, A., Budowle, B., 2016. Expansion of microbial forensics. J. Clin. Microbiol. 54, 1964–1974.
Schroeder, H., Ávila-Arcos, M.C., Malaspinas, A.-S., Poznik, G.D., Sandoval-Velasco, M., Carpenter, M.L., Moreno-Mayar, J.V., Sikora, M., Johnson, P.L., Allentoft, M.E., 2015. Genome-wide ancestry of 17th-century enslaved Africans from the Caribbean. Proc. Natl. Acad. Sci. 201421784.
Schubert, M., Ermini, L., Sarkissian, C.D., Jónsson, H., Ginolhac, A., Schaefer, R., Martin, M.D., Fernández, R., Kircher, M., McCue, M., Willerslev, E., Orlando, L., 2014. Characterization of ancient and modern genomes by SNP detection and phylogenomic and metagenomic analysis using PALEOMIX. Nat. Protoc. 9, 1056–1082. https://doi.org/10.1038/nprot.2014.063
Schubert, M., Lindgreen, S., Orlando, L., 2016. AdapterRemoval v2: rapid adapter trimming, identification, and read merging. BMC Res. Notes 9, 88.
Schuster, S.C., 2007. Next-generation sequencing transforms today's biology. Nat. Methods 5, 16.
Seguin-Orlando, A., Korneliussen, T.S., Sikora, M., Malaspinas, A.-S., Manica, A., Moltke, I., Albrechtsen, A., Ko, A., Margaryan, A., Moiseyev, V., 2014. Genomic structure in Europeans dating back at least 36,200 years. Science 346, 1113–1118.
Simón-Soro, A., Mira, A., 2015. Solving the etiology of dental caries. Trends Microbiol. 23, 76–82.
Soltis, P.S., Soltis, D.E., Smiley, C.J., 1992. An rbcL sequence from a Miocene Taxodium (bald cypress). Proc. Natl. Acad. Sci. 89, 449–451.
Spence, M.W., Pereira, G., 2007. The human skeletal remains of the Moon Pyramid, Teotihuacan. Anc. Mesoam. 18, 147–157.
Steven, B., Niederberger, T.D., Whyte, L.G., 2009. Bacterial and Archaeal Diversity in Permafrost, in: Margesin, R. (Ed.), Permafrost Soils, Soil Biology. Springer Berlin Heidelberg, Berlin, Heidelberg, pp. 59–72. https://doi.org/10.1007/978-3-540-69371-0_5
Stoneking, M., 1995. Ancient DNA: how do you know when you have it and what can you do with it? Am. J. Hum. Genet. 57, 1259.
Struzycka, I., 2014. The oral microbiome in dental caries. Pol. Microbiol. 63, 127–135.
Sugiyama, N., Somerville, A.D., Schoeninger, M.J., 2015. Stable isotopes and zooarchaeology at Teotihuacan, Mexico reveal earliest evidence of wild carnivore management in Mesoamerica. PloS One 10, e0135635.
Sugiyama, N., Sugiyama, S., Ortega, V., Fash, W., 2016. Plaza of the Columns at Teotihuacan: Scope, Goals and Expectations of a New International Project. Presented at the Society for American Archaeology 81st Annual Meeting, Orlando, Florida.
Sugiyama, S., Cabrera, R., López, L., 2004. The Moon Pyramid Burials. Voyage Cent. Moon Pyramid Recent Discov. Teotihuacan 20–30.
Sugiyama, S., Castro, R.C., 2007. The Moon Pyramid project and the Teotihuacan state polity: A brief summary of the 1998–2004 excavations. Anc. Mesoam. 18, 109–125.
Sugiyama, S., Luján, L.L., 2007. DEDICATORY BURIAL/OFFERING COMPLEXES AT THE MOON PYRAMID, TEOTIHUACAN: A preliminary report of 1998–2004 explorations. Anc. Mesoam. 18, 127–146. https://doi.org/10.1017/S0956536107000065
Suzuki, M.T., Giovannoni, S.J., 1996. Bias caused by template annealing in the amplification of mixtures of 16S rRNA genes by PCR. Appl Env. Microbiol 62, 625–630.
Taube, K.A., 2005. The symbolism of jade in Classic Maya religion. Anc. Mesoam. 16, 23–50.

Tirosh, O., Conlan, S., Deming, C., Lee-Lin, S.-Q., Huang, X., Su, H.C., Freeman, A.F., Segre, J.A., Kong, H.H., 2018. Expanded skin virome in DOCK8-deficient patients. Nat. Med. 24, 1815.

Tito, R.Y., Knights, D., Metcalf, J., Obregon-Tito, A.J., Cleeland, L., Najar, F., Roe, B., Reinhard, K., Sobolik, K., Belknap, S., 2012. Insights from characterizing extinct human gut microbiomes. PloS One 7, e51146.

Turnbaugh, P.J., Ley, R.E., Hamady, M., Fraser-Liggett, C.M., Knight, R., Gordon, J.I., 2007. The Human Microbiome Project. Nature 449, 804–810. https://doi.org/10.1038/nature06244

V. Wintzingerode, F., Göbel, U.B., Stackebrandt, E., 1997. Determination of microbial diversity in environmental samples: pitfalls of PCR-based rRNA analysis. FEMS Microbiol. Rev. 21, 213–229. https://doi.org/10.1111/j.1574-6976.1997.tb00351.x

Velsko, I.M., Frantz, L.A.F., Herbig, A., Larson, G., Warinner, C., 2018. Selection of Appropriate Metagenome Taxonomic Classifiers for Ancient Microbiome Research. mSystems 3, e00080-18. https://doi.org/10.1128/mSystems.00080-18

Wade, W.G., 2013. The oral microbiome in health and disease. Pharmacol. Res. 69, 137–143.

Warinner, C., Herbig, A., Mann, A., Fellows Yates, J.A., Weiß, C.L., Burbano, H.A., Orlando, L., Krause, J., 2017. A robust framework for microbial archaeology. Annu. Rev. Genomics Hum. Genet. 18, 321–356.

Warinner, C., Rodrigues, J.F.M., Vyas, R., Trachsel, C., Shved, N., Grossmann, J., Radini, A., Hancock, Y., Tito, R.Y., Fiddyment, S., 2014. Pathogens and host immunity in the ancient human oral cavity. Nat. Genet. 46, 336.

Warinner, C., Speller, C., Collins, M.J., 2015. A new era in palaeomicrobiology: prospects for ancient dental calculus as a long-term record of the human oral microbiome. Phil Trans R Soc B 370, 20130376.

Weyrich, L.S., Duchene, S., Soubrier, J., Arriola, L., Llamas, B., Breen, J., Morris, A.G., Alt, K.W., Caramelli, D., Dresely, V., Farrell, M., Farrer, A.G., Francken, M., Gully, N., Haak, W., Hardy, K., Harvati, K., Held, P., Holmes, E.C., Kaidonis, J., Lalueza-Fox, C., de la Rasilla, M., Rosas, A., Semal, P., Soltysiak, A., Townsend, G., Usai, D., Wahl, J., Huson, D.H., Dobney, K., Cooper, A., 2017. Neanderthal behaviour, diet, and disease inferred from ancient DNA in dental calculus. Nature 544, 357–361. https://doi.org/10.1038/nature21674

Woodward, Weyand, N.J., Bunnell, M., 1994. DNA sequence from Cretaceous period bone fragments. Science 266, 1229–1232. https://doi.org/10.1126/science.7973705

Zaura, E., Nicu, E.A., Krom, B.P., Keijser, B.J., 2014. Acquiring and maintaining a normal oral microbiome: current perspective. Front. Cell. Infect. Microbiol. 4, 85.

Zhou, Y., Gao, H., Mihindukulasuriya, K.A., La Rosa, P.S., Wylie, K.M., Vishnivetskaya, T., Podar, M., Warner, B., Tarr, P.I., Nelson, D.E., 2013. Biogeography of the ecosystems of the healthy human body. Genome Biol. 14, R1.

Ziesemer, K.A., Mann, A.E., Sankaranarayanan, K., Schroeder, H., Ozga, A.T., Brandt, B.W., Zaura, E., Waters-Rist, A., Hoogland, M., Salazar-García, D.C., 2015. Intrinsic challenges in ancient microbiome reconstruction using 16S rRNA gene amplification. Sci. Rep. 5, 16498.

Ziesemer, K.A., Ramos-Madrigal, J., Mann, A.E., Brandt, B.W., Sankaranarayanan, K., Ozga, A.T., Hoogland, M., Hofman, C.A., Salazar-García, D.C., Frohlich, B., Milner, G.R., Stone, A.C., Aldenderfer, M., Lewis, C.M., Hofman, C.L., Warinner, C., Schroeder, H., 2019. The efficacy of whole human genome capture on ancient dental calculus and dentin. Am. J. Phys. Anthropol. 168, 496–509. https://doi.org/10.1002/ajpa.23763

Appendix A

Table A.1: Sample metadata

Sample ID/Source Accession Number	Total Number of Reads	Locality	Environment	Instrument	Description
ElSidron1	56,584,638	Spain	Calculus	Illumina HiSeq	Weyrich_etal_2017
ElSidron2	66,905,980	Spain	Calculus	Illumina MiSeq 300	Weyrich_etal_2017
OldSpy	69,901,550	Belgium	Calculus	Illumina MiSeq 300	Weyrich_etal_2017
SRR6877282	19,199,306	Nepal	Calculus	Illumina HiSeq 2500	Mann_etal_2018
SRR6877284	44,932,086	Spain	Calculus	Illumina HiSeq 2500	Mann_etal_2018
SRR6877286	16,562,372	Spain	Calculus	Illumina HiSeq 2500	Mann_etal_2018
SRR6877288	22,746,512	Guadeloupe	Calculus	Illumina HiSeq 2500	Mann_etal_2018
SRR6877290	18,595,784	Guadeloupe	Calculus	Illumina HiSeq 2500	Mann_etal_2018
SRR6877292	27,888,566	Mongolia	Calculus	Illumina HiSeq 2500	Mann_etal_2018
SRR6877312	11,561,738	USA	Calculus	Illumina HiSeq 2500	Mann_etal_2018
SRR6877310	11,945,018	USA	Calculus	Illumina HiSeq 2500	Mann_etal_2018
SRR6877393	14,907,918	Netherlands	Calculus	Illumina HiSeq 2500	Mann_etal_2018
ERR011323	12,479,816	Spain	Human Gut	IlluminaGenomeAnalyzerII	Ormerod_etal_2016
ERR2162202	20,813,974	USA	Human Gut	Illumina_HiSeq_2000	Gopalakrishnan_etal_2018
ERR2162205	21,616,115	USA	Human Gut	Illumina_HiSeq_2000	Gopalakrishnan_etal_2018
ERR2162208	18,979,022	USA	Human Gut	Illumina_HiSeq_2000	Gopalakrishnan_etal_2018
ERR2162209	20,006,202	USA	Human Gut	Illumina_HiSeq_2000	Gopalakrishnan_etal_2018
ERR2162211	19,724,770	USA	Human Gut	Illumina_HiSeq_2000	Gopalakrishnan_etal_2018
ERR2162212	19,119,666	USA	Human Gut	Illumina_HiSeq_2000	Gopalakrishnan_etal_2018
ERR2162215	18,234,407	USA	Human Gut	Illumina_HiSeq_2000	Gopalakrishnan_etal_2018
ERR2162216	21,516,313	USA	Human Gut	Illumina_HiSeq_2000	Gopalakrishnan_etal_2018
ERR2162220	17,308,536	USA	Human Gut	Illumina_HiSeq_2000	Gopalakrishnan_etal_2018
ERR2162221	18,980,740	USA	Human Gut	Illumina_HiSeq_2000	Gopalakrishnan_etal_2018
ERR321065	11,165,183	Denmark	Human Gut	IlluminaGenomeAnalyzerII	Costea_etal_2017
SRR1929408	31,843,136	Tanzania	Human Gut	IlluminaGenomeAnalyzerIIx	Rampelli_etal_2017
SRR1930121	35,645,325	Tanzania	Human Gut	IlluminaGenomeAnalyzerIIx	Rampelli_etal_2017
SRR1930123	3,732,121	Tanzania	Human Gut	IlluminaGenomeAnalyzerIIx	Rampelli_etal_2017
SRR1930141	32,369,669	Tanzania	Human Gut	IlluminaGenomeAnalyzerIIx	Rampelli_etal_2017
SRR1930145	16,695,141	Tanzania	Human Gut	IlluminaGenomeAnalyzerIIx	Rampelli_etal_2017

SRR1931170	16,744,111	Italy	Human Gut	IlluminaGenomeAnalyzerIIx	Rampelli_etal_2017
SRR1931173	23,917,309	Italy	Human Gut	IlluminaGenomeAnalyzerIIx	Rampelli_etal_2017
SRR1952513	32,056,125	Australia	Plaque	Illumina_HiSeq_2000	Lloyd.Price_etal_2017
SRR1952567	32,453,927	Australia	Plaque	Illumina_HiSeq_2000	Lloyd.Price_etal_2017
SRR1952611	28,677,800	Australia	Plaque	Illumina_HiSeq_2000	Lloyd.Price_etal_2017
SRR1952623	42,484,177	Australia	Plaque	Illumina_HiSeq_2000	Lloyd.Price_etal_2017
SRR2240834	28,592,053	Australia	Plaque	Illumina_HiSeq_2000	Lloyd.Price_etal_2017
SRR2240920	27,386,137	Australia	Plaque	Illumina_HiSeq_2000	Lloyd.Price_etal_2017
SRR3586059	16,735,210	USA	Plaque	Illumina_HiSeq_1000	Schmidt_etal_2014
SRR3586060	47,986,616	USA	Plaque	Illumina_HiSeq_1000	Schmidt_etal_2014
SRR3586063	12,545,392	USA	Plaque	Illumina_HiSeq_1000	Schmidt_etal_2014
SRR3586064	14,935,707	USA	Plaque	Illumina_HiSeq_1000	Schmidt_etal_2014
ERR1474568	41,891,239	Philippines	Saliva	Illumina_HiSeq_2500	Lassalle_etal_2017
ERR1474580	33,510,069	Philippines	Saliva	Illumina_HiSeq_2500	Lassalle_etal_2017
ERR1474585	18,384,662	Philippines	Saliva	Illumina_HiSeq_2500	Lassalle_etal_2017
ERR1474586	40,615,282	Philippines	Saliva	Illumina_HiSeq_2500	Lassalle_etal_2017
SRR7448290	33,977,611	USA	Saliva	NextSeq500	Aleti_etal_2018
SRR7448291	31,509,401	USA	Saliva	NextSeq500	Aleti_etal_2018
SRR7448292	16,188,903	USA	Saliva	NextSeq500	Aleti_etal_2018
SRR7448294	18,614,551	USA	Saliva	NextSeq500	Aleti_etal_2018
SRR7448307	116,315,187	USA	Saliva	NextSeq500	Aleti_etal_2018
SRR7448312	27,142,636	USA	Saliva	NextSeq500	Aleti_etal_2018
SRR1620017	29,006,012	USA	Skin	Illumina_HiSeq_2000	Schmedes_etal_2017
SRR3644405	10,783,066	USA	Skin	Illumina_HiSeq_2000	Loshcher_etal_2015
SRR7687997	16,588,845	USA	Skin	Illumina_HiSeq_2500	Tirosh_etal_2018
SRR7992620	21,406,093	USA	Skin	Illumina_HiSeq_2500	Tirosh_etal_2018
SRR7992621	20,812,370	USA	Skin	Illumina_HiSeq_2500	Tirosh_etal_2018
SRR7992810	15,142,399	USA	Skin	Illumina_HiSeq_2500	Tirosh_etal_2018
ERR2004605	21,032,723	China	Soil	NextSeq500	Ren_etal_2018
ERR2004609	20,618,976	China	Soil	NextSeq500	Ren_etal_2018
ERR2004615	20,997,843	China	Soil	NextSeq500	Ren_etal_2018
SRR1157607	27,629,264	USA	Soil	Illumina_HiSeq_2000	Lin_etal_2014
SRR1157609	52,421,485	USA	Soil	Illumina_HiSeq_2000	Lin_etal_2014
SRR5277367	67,906,864	Canada	Soil	Illumina_HiSeq_2500	DOE_2017
SRR8465122	7,302,341	Norway	Soil	Illumina_HiSeq_2500	DOE_2017
SRR8465471	7,403,704	Norway	Soil	Illumina_HiSeq_2500	DOE_2017